

Polimery w Medycynie

Polymers in Medicine

BIANNUAL ISSN: 0370-0747 e-ISSN: 2451-2699

www.polimery.umed.wroc.pl

2018, Vol. 48, No. 2 (July–December)

Ministry of Science and Higher Education – 9 pts.
Index Copernicus (ICV) – 109.18 pts.



WROCLAW
MEDICAL UNIVERSITY

Polimery w Medycynie

Polymers in Medicine

ISSN 0370-0747 (PRINT)

ISSN 2451-2699 (ONLINE)

www.polimery.umed.wroc.pl

BIANNUAL
2018, Vol. 48, No. 2
(July–December)

“Polymers in Medicine” is an independent, multidisciplinary forum to exchange scientific and clinical information, which publishes original papers (technical, analytical, experimental, clinical), preliminary reports and reviews regarding the use of polymers (natural and synthetic) and biomaterials in different specialties of medicine (biochemistry, clinical medicine, pharmacology, dentistry, implantology), biotechnology and veterinary science.

Address of Editorial Office

Marcinkowskiego 2–6
50-368 Wrocław, Poland
Tel.: +48 71 784 11 33
E-mail: polimery@umed.wroc.pl

Publisher

Wrocław Medical University
Wybrzeże L. Pasteura 1
50-367 Wrocław, Poland

© Copyright by Wrocław Medical University,
Wrocław 2019

Online edition is the original version of the journal

Editor-in-Chief

Magdalena Krajewska
Mariusz Kuształ

Vice-Editor-in-Chief

Jerzy Gosk

Editorial Board

Rajmund Adamiec
Beata Dejak
Bożena Karolewicz
Witold Musiał

Thematic Editors

Bożena Karolewicz
(Multifunctional polymers in pharmaceutical technology and medical applications)
Witold Musiał
(Physicochemical evaluation of polymers used in pharmacy and medicine)
Agnieszka Wojciechowska
(Bioinorganic chemistry and coordination chemistry)
Agnieszka Noszczyk-Nowak
(Experimental research)

International Advisory Board

Jennifer B. Dressman (Germany)
Mirosława El Fray (Poland)
Mukesh G. Gohel (India)
Vipin B. Gupta (India)
Anthony J. Hickey (USA)
Jacek Kaczmarczyk (Poland)

Secretary

Maciej Szymczak

Michał Nachajski
Tadeusz Orłowski
Lidia Usnarska-Zubkiewicz
Włodzimierz Więckiewicz

Technical Editorship

Adam Barg, Marek Misiak,
Aleksandra Raczkowska

Statistical Editors

Dorota Diakowska, Leszek Noga

English Language Copy Editors

Jason Schock, Marcin Tereszewski,
Sherill Howard Pocięcha

Agnieszka Noszczyk-Nowak (Poland)
Paweł Reichert (Poland)
Maciej Urban (Poland)
Timothy S. Wiedmann (USA)
Katarzyna Winnicka (Poland)
Waldemar Wysokiński (USA)
Samuel Yalkowsky (USA)

Editorial Policy

During the review process, the Editorial Board conforms to the "Uniform Requirements for Manuscripts Submitted to Biomedical Journals: Writing and Editing for Biomedical Publication" approved by the International Committee of Medical Journal Editors (<http://www.icmje.org/>). Experimental studies must include a statement that the experimental protocol and informed consent procedure were in compliance with the Helsinki Convention and were approved by the ethics committee.

For more information visit the following page: <http://www.polimery.umed.wroc.pl>

Indexed in: OCLC, WorldCat, PBL, EBSCO, MEDLINE, Index Copernicus

This publication has been co-financed by the Ministry of Science and Higher Education

Typographic design: Monika Kołęda, Piotr Gil

Cover: Monika Kołęda

DTP: Wrocław Medical University Press

Printing and binding: EXDRUK

Circulation: 11 copies

Polimery w Medycynie

Polymers in Medicine

BIENNIAL 2018, Vol. 48, No. 2 (July–December)

ISSN 0370-0747 (PRINT)
ISSN 2451-2699 (ONLINE)
www.polimery.umed.wroc.pl

Contents

- 69 Abid Mehmood Yousaf, Sundas Zulfiqar, Yasser Shahzad, Talib Hussain, Tariq Mahmood, Muhammad Jamshaid
The preparation and physicochemical characterization of eprosartan mesylate-laden polymeric ternary solid dispersions for enhanced solubility and dissolution rate of the drug
- 77 Marta Karaźniewicz-Łada, Karina Bąba, Filip Dolatowski, Alicja Dobrowolska, Marlena Rakicka
The polymorphism of statins and its effect on their physicochemical properties
- 83 Magdalena Domosławska, Renata Pawlak-Morka, Łukasz Dobrzyński, Monika Herda
Study of the influence of cellulose derivatives on physical and analytical attributes of a drug product belonging to BCS class II
- 91 Olubusola A. Odeniyi, David S. Avoseh
Effects of media components and agricultural by-products on γ -polyglutamic acid production by *Bacillus toyonensis* As8
- 99 Jyotsana R. Madan, Rishikesh H. Dagade, Rajendra Awasthi, Kamal Dua
Formulation and solid state characterization of carboxylic acid-based co-crystals of tinidazole: An approach to enhance solubility

The preparation and physicochemical characterization of eprosartan mesylate-laden polymeric ternary solid dispersions for enhanced solubility and dissolution rate of the drug

Abid Mehmood Yousaf^{1,A,C,D}, Sundas Zulfiqar^{2,B}, Yasser Shahzad^{1,C,E}, Talib Hussain^{1,E}, Tariq Mahmood^{2,C,E}, Muhammad Jamshaid^{2,F}

¹ Department of Pharmacy, COMSATS University Islamabad, Lahore Campus, Pakistan

² Faculty of Pharmacy, University of Central Punjab, Lahore, Pakistan

A – research concept and design; B – collection and/or assembly of data; C – data analysis and interpretation;

D – writing the article; E – critical revision of the article; F – final approval of the article

Polymers in Medicine, ISSN 0370-0747 (print), ISSN 2451-2699 (online)

Polim Med. 2018;48(2):69–75

Address for correspondence

Abid Yousaf

E-mail: abid.ucp@hotmail.com

Funding sources

None declared

Conflict of interest

None declared

Acknowledgements

The authors are thankful to the University of Central Punjab and to the COMSATS University Islamabad for providing all the materials and the laboratory facility for this research.

Received on April 19, 2018

Reviewed on December 5, 2018

Accepted on January 16, 2019

Cite as

Tousaf AM, Zulfiqar S, Shahzad Y, Hussain T, Mahmood T, Jamshaid M. The preparation and physicochemical characterization of eprosartan mesylate-laden polymeric ternary solid dispersions for enhanced solubility and dissolution rate of the drug. *Polim Med.* 2018;48(2):69–75. doi:10.17219/pim/102976

DOI

10.17219/pim/102976

Copyright

© 2019 by Wrocław Medical University

This is an article distributed under the terms of the

Creative Commons Attribution Non-Commercial License

(<http://creativecommons.org/licenses/by-nc-nd/4.0/>)

Abstract

Background. Eprosartan mesylate is a poorly water-soluble drug. It does not dissolve well in the aqueous gastrointestinal fluid, which means it is not absorbed well via the oral route, because a drug can cross cell membranes when it is dissolved in the gastrointestinal fluid.

Objectives. The purpose of this research was to enhance the aqueous solubility and dissolution rate of eprosartan mesylate using the solid dispersion technique. Enhancing the solubility and dissolution leads to better absorption via the oral route.

Material and methods. A number of eprosartan mesylate-laden polymeric solid dispersions were prepared with hydroxypropyl methylcellulose (HPMC) and polysorbate 80 by means of the solvent evaporation technique. The impact of the weight ratios of the constituents on the solubility and dissolution rate was studied in comparison with the plain drug. The formulation presenting the optimal solubility and dissolution underwent the solid-state characterization using X-ray diffraction (XRD), differential scanning calorimetry (DSC), scanning electron microscopy (SEM), and Fourier-transform infrared spectroscopy (FTIR).

Results. Both polysorbate 80 and HPMC positively affected the solubility and dissolution of eprosartan mesylate.

Conclusions. In particular, a ternary solid dispersion consisting of eprosartan mesylate, HPMC and polysorbate 80 at a weight ratio of 1:4.2:0.3 showed the highest solubility (36.39 ± 3.95 mg/mL) and dissolution ($86.19 \pm 4.09\%$ in 10 min). Moreover, the drug was present in the amorphous form in the solid dispersion with no covalent drug–excipient interactions.

Key words: amorphous, hydroxypropyl methylcellulose, aqueous solubility, eprosartan mesylate, polymeric solid dispersions

Introduction

Eprosartan mesylate, a monomethanesulfonate of (*E*)-2-butyl-1-(*p*-carboxybenzyl)- α -2-thienylmethylimidazole-5-acrylic acid,¹ is a water-insoluble crystalline powder.² It is considered a promising angiotensin II receptor antagonist.³ It is usually prescribed at a dose of 400–800 mg once or twice daily for 13 weeks to patients with mild to severe hypertension.⁴ Unlike angiotensin-converting enzyme inhibitors, it does not induce coughing and has no severe drug interactions.⁵

As a poorly water-soluble drug (its solubility in water is <1 mg/mL at 25°C), eprosartan mesylate is categorized in class 2 of the Biopharmaceutics Classification System (BCS). The oral bioavailability of a BCS class 2 drug can be enhanced by ameliorating its aqueous solubility using a solubility-enhancing technique such as solid dispersion.⁶ As its efficacy is very low, eprosartan mesylate is administered in high doses.^{7,8} Improving the solubility of eprosartan mesylate in water might improve its oral efficacy and circumvent the need for high doses.

Several techniques, such as micronization, nanoparticle formation, solubilization with surfactants, microemulsions, complexation with cyclodextrins, encapsulation with hydrophilic polymeric wall materials, self-emulsifying drug delivery systems, and dispersing hydrophobic drugs in hydrophilic polymeric matrices, have been successfully employed to improve the aqueous solubility and dissolution of poorly water-soluble drugs.

Solid dispersion – the dispersal of a hydrophobic drug in a hydrophilic polymer with or without the addition of a surfactant – is an excellent strategy to enhance the solubility and dissolution of water-insoluble drugs.^{9–19} A solid dispersion prepared with the addition of a surfactant (a ternary solid dispersion) results in greater improvement of the solubility and dissolution of BCS class 2 drugs as compared to solid dispersions prepared without a surfactant (binary solid dispersions).²⁰ Solid dispersions can be prepared conventionally by the melting method,²¹ the kneading method,²² the solvent evaporation method,⁹ or the lyophilization technique.²³ The use of solid dispersions manufactured by the solvent evaporation method is among the most promising ways to enhance the solubility and dissolution rates of water-insoluble chemical entities, due to the molecular-level closeness of the drug to the hydrophilic carriers, which improves wetting, and the conversion of the crystalline components into their respective amorphous forms, which enhances the surface area exposed to the surrounding dissolution medium.^{18,24}

In the present study, a number of eprosartan mesylate-laden ternary solid dispersions were prepared with hydroxypropyl methylcellulose (HPMC) and polysorbate 80 by the solvent evaporation method. The aqueous solubility and dissolution of the drug in the solid dispersions were determined. The structural, thermal, morphological, and spectroscopic characteristics of the solid disper-

sion exhibiting the best solubility and dissolution were determined using X-ray diffraction (XRD), differential scanning calorimetry (DSC), scanning electron microscopy (SEM), and Fourier-transform infrared spectroscopy (FTIR), respectively.

Material and methods

Material

Eprosartan mesylate was supplied by the Jinan Chenghui-Shuangda Chemical Co., Ltd. (Jinan, China). Polyvinylpyrrolidone (PVP), sodium lauryl sulfate (SLS), carboxymethylcellulose sodium (CMC-Na), and 2-hydroxypropyl-beta-cyclodextrin (HP- β -CD) were from Sigma-Aldrich (St. Louis, USA). Poly-oxyethylene esters of 12-hydroxystearic acid (Solutol[®] HS 15), poloxamer 188 and poloxamer 407 were procured from BASF (Ludwigshafen am Rhein, Germany). Gelatin, polyethylene glycol 6000 (PEG-6000), polysorbate 20 (tween 20), polysorbate 60 (tween 60), polysorbate 80 (tween 80), sorbitan mono-laurate 20 (span 20), and sorbitan monooleate 80 (span 80) were obtained from Daejung Chemicals & Metals Co., Ltd. (Siheung, South Korea). Hydroxypropyl methylcellulose and dextran were bought from Shin-Etsu Chemical Co., Ltd. (Tokyo, Japan). Carbopol[®] 941 was from Lubrizol Corp. (Wickliffe, USA). All other materials were of the reagent grade.

Method of preparation

For each solid dispersion formulation, exactly weighed amounts of eprosartan mesylate, HPMC and polysorbate 80 were completely dissolved in 80% (v/v) aqueous ethanol to make a transparent solution. These solutions were dried in a tray dryer at 40°C until a constant weight was achieved. The dried mass was pulverized and passed through a sieve 60. The solid dispersions were stored in an air-tight 45-milliliter conical tube. The composition of the various solid dispersions is shown in Table 1.

Table 1. The compositions (w/w/w) of the eprosartan mesylate-laden polymeric solid dispersions used in the study

Components [g]	I	II	III	IV	V	VI	VII
Eprosartan mesylate	1.0	1.0	1.0	1.0	1.0	1.0	1.0
HPMC	1.0	0.9	0.8	0.7	2.1	4.2	5.6
Polysorbate 80	0	0.1	0.2	0.3	0.3	0.3	0.3

HPMC – hydroxypropyl methylcellulose.

Solubility test

Excess of the solid dispersion was added to 1 mL of distilled water in a 2-milliliter microtube and vortexed for 1 min. Each sample was placed in a water bath (25°C) and agitated (100 rpm) for 5 days. Then, after centrifugation

(5000 g), 0.5 mL of the supernatant was carefully taken using a micropipette and appropriately diluted with ethanol. The diluent was analyzed using a HALO DB-20 UV-visible spectrophotometer (Dynamica Scientific, Ltd., Clayton, Australia) at a wavelength of 233 nm to determine the concentration of eprosartan mesylate.

Drug content determination

For each formulation, a carefully weighed quantity, equivalent to 50 mg of eprosartan mesylate, was dissolved in 100 mL of 80% (v/v) aqueous ethanol in a 100-milliliter measuring flask. Thus, the theoretical concentration of the stock solution was 500 µg/mL. The solution was strained through a 0.45 µm pore-sized syringe filter and the filtrate was diluted appropriately with ethanol. Then, using the HALO DB-20 UV-visible spectrophotometer, the diluted sample was analyzed at a wavelength of 233 nm to calculate the concentration of eprosartan mesylate. The experiment was carried out in triplicate for each formulation. The eprosartan mesylate content was determined by the following formula:

$$X_s = X_a / X_t \times 100 \quad (1)$$

where

X_s – the content of eprosartan mesylate [%];

X_a – the actual titer, quantified through the UV-visible spectrophotometer [µg/mL];

X_t – the theoretical concentration [µg/mL].

Dissolution test

Dissolution was investigated using a USP Dissolution Apparatus 2 (Vision® Classic 6™; Hanson Research Corp., Los Angeles, USA). Each sample, equivalent to 50 mg of eprosartan mesylate, was added to 900 mL of a dissolution medium containing 1% (w/v) SLS.^{25,26} The dissolution medium was kept at 37 ± 0.5°C by a surrounding water bath. The paddle was fixed at a rotation speed of 100 rpm.¹⁹ At each predetermined time point, 1 mL of the dissolution medium was sampled, filtered (a pore size of 0.45 µm) and diluted adequately. After each sampling, the dissolution medium was immediately replenished with the pre-warmed dissolution medium to maintain the sink conditions. The diluted samples were examined by the HALO DB-20 UV-visible spectrophotometer at a wavelength of 233 nm.

Powder X-ray diffraction

The crystallinity or amorphousness of the samples was assessed using a Rigaku X-ray diffractometer (D/MAX-2500 PC; Rigaku Corp., Tokyo, Japan). The X-ray diffraction analysis was completed using the Cu $K\alpha_1$ monochromatic radiation source at a voltage of 50 kV and a current

of 100 mA. The powder XRD (PXRD) results were recorded in the 10–70° range in the 2θ scanning mode, at a scan speed of 5°/min and a step size of 0.02°/s.

Differential scanning calorimetry

Differential scanning calorimetry was used as a confirmatory test for the change of the crystalline form of eprosartan mesylate to the amorphous form in the optimal formulation. Hydroxypropyl methylcellulose, the eprosartan mesylate powder, a physical blend and the optimized solid dispersion formulation were analyzed using a differential scanning calorimeter DSC Q20 (TA Instruments, New Castle, USA). The physical mixture was obtained by mixing eprosartan mesylate, HPMC and polysorbate 80, in the same weight ratio as in the optimal formulation, using a mortar and a pestle. About 10 mg of each sample was tightly enclosed in the aluminum sample pan and heated at 15°C/min in the calorimeter. The test was executed in the range of 30–300°C in the presence of nitrogen gas flowing at a rate of 30 mL/min.

Scanning electron microscopy

The evaluation of the morphology of the pure eprosartan mesylate powder, HPMC and the optimal solid dispersion was performed using an S-4800 scanning electron microscope (Hitachi, Ltd., Tokyo, Japan). All the samples were coated with platinum and inspected under the electron microscope. Platinum coating is necessary for proper visibility and imaging of the samples; without it, samples are either invisible or extremely blurry.

Fourier-transform infrared spectroscopy

A Nicolet 6700 spectrophotometer (Thermo Fisher Scientific, Inc., Waltham, USA) was used for the FTIR analyses of the optimal formulation, the physical mixture and the individual components. Each sample was appropriately mounted on the sample disc under the scanning pin and viewed from 600 cm⁻¹ to 4000 cm⁻¹ using a resolution of 2 cm⁻¹.

Statistical methods

In the solubility test, 3 samples were analyzed for each polymer, surfactant and formulation. The mean value and standard deviation (SD) were determined using MS Excel software (Microsoft Corp., Redmond, USA). During the dissolution test, 6 samples were taken at specified time points for each formulation, and the mean value and SD were determined. Moreover, values of percent dissolved obtained at a specific time point for the optimal formulation were compared with the corresponding values of each formulation separately, using the t-test. A p-value of 0.05 was taken as the threshold of statistical significance.

Results and discussion

First, to select the most appropriate excipients for a ternary solid dispersion, the solubility of eprosartan mesylate was determined in 1% (w/v) aqueous solutions of each surfactant and hydrophilic polymer. The hydrophilic polymer and surfactant in which the drug exhibited the highest apparent solubility were selected for the preparation of solid dispersions. Eprosartan mesylate showed the highest solubility in HPMC (514.43 ± 3.53 µg/mL) and polysorbate 80 (513.64 ± 0.12 µg/mL) among the polymers and surfactants, respectively; therefore, they were selected as the most appropriate constituents for the solid dispersion formulation in this study (Fig. 1A and 1B, respectively).

The solvent evaporation method is considered one of the most promising methods for the preparation of solid dispersions in terms of the enhancement of solubility,

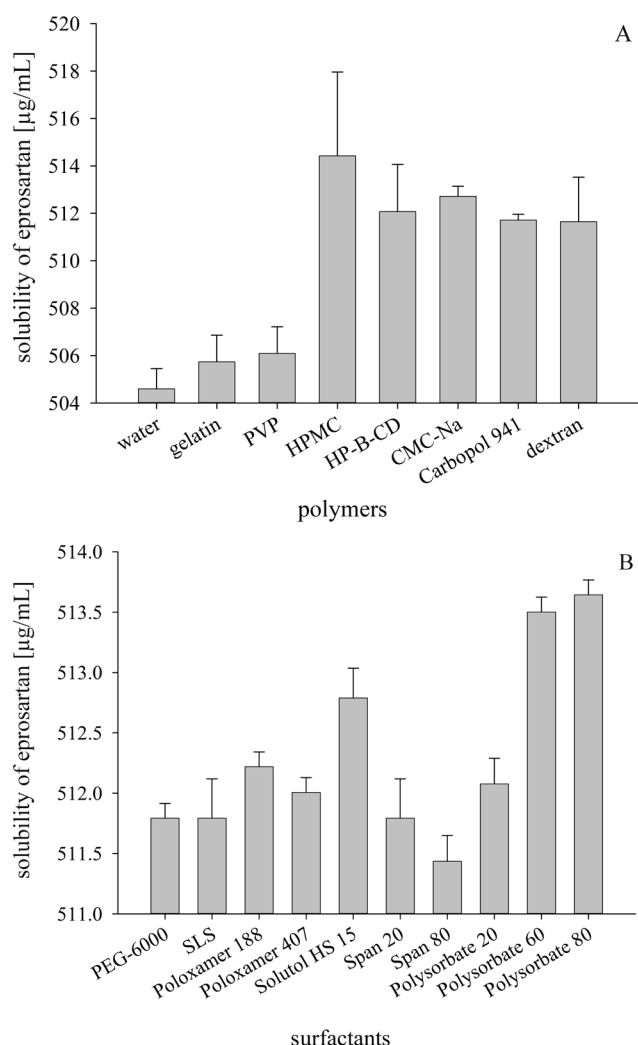


Fig. 1. The solubility of eprosartan mesylate in 1% (w/v) aqueous solution of various carriers: hydrophilic polymers (A) and surfactants (B). Each value denotes the mean ± standard deviation (SD) of 3 trials

CMC-Na – carboxymethylcellulose sodium; HP-β-CD – 2-hydroxypropyl-beta-cyclodextrin; PEG-6000 – polyethylene glycol 6000; PVP – polyvinylpyrrolidone; SLS – sodium lauryl sulfate; Solutol HS 15 – poly-oxyethylene esters of 12-hydroxystearic acid; span 20 – sorbitan monolaurate 20; span 80 – sorbitan monooleate 80.

dissolution and oral bioavailability.^{9,18} In this method, the drug and the excipients are completely dissolved in a solvent before drying to achieve molecular-level mixing. Therefore, all the components are homogeneously present and closely combined in the dried product. This improves wetting and enhances the surface area of the drug by converting it to its amorphous counterpart, as the polymeric matrix prevents the recrystallization of the drug. Normally, during the drying process, the dissolved crystalline drug tends to recrystallize from the solution,²⁷ but this tendency is inhibited when polymeric matrices are present in the solution.^{28,29} In such cases, recrystallization is either circumvented completely or crystalline intensity is diminished considerably.^{18,27} Both the type³⁰ and quantity^{31,32} of the polymeric matrix play a role in exerting this inhibitory effect on recrystallization. The homogeneity of the products was reflected by the high drug content, which was 99–101% in all formulations in this study. The solvent evaporation method was therefore adopted in our study.

All the 7 formulations showed better solubility and dissolution than plain eprosartan mesylate (Fig. 2A and 2B, respectively). The solubility for each formulation was as follows: I – 3.06 ± 0.80 mg/mL; II – 7.69 ± 1.93 mg/mL; III – 14.25 ± 4.11 mg/mL; IV – 23.00 ± 3.34 mg/mL; V – 34.98 ± 3.42 mg/mL; VI – 36.39 ± 3.95 mg/mL; and VII – 32.01 ± 3.92 mg/mL. The dissolution at 10 min was: I – 8.94 ± 0.70%; II – 23.95 ± 3.87%; III – 35.40 ± 3.57%; IV – 55.27 ± 8.02%; V – 85.48 ± 10.16%; VI – 86.19 ± 4.09%; and VII – 84.24 ± 5.20%. As the quantity of the surfactant increased in formulations I–IV, the solubility and dissolution were improved. This enhanced solubility can be accredited to the solubilizing power of polysorbate 80. Formulation IV was then selected, and the further effect of HPMC on solubility and dissolution was investigated. Hydroxypropyl methylcellulose improved the aqueous solubility and dissolution as compared to formulation IV. This further improvement can be ascribed to the hydrophilic polymer increasing the wettability of the drug. In particular, formulation VI showed the highest solubility and dissolution; however, the values of formulations V–VII did not significantly differ from one another. The solubility of formulation VI was also higher than the solubility of the corresponding physical mixture (36.39 ± 3.95 mg/mL vs 19.98 ± 7.98 mg/mL, respectively). Moreover, the dissolution rate of eprosartan mesylate with solid dispersion formulation VI was more rapid than the rates achieved by the solid dispersions discussed in some recent studies.^{33,34} As compared to formulation VI, the dissolution profile of the corresponding physical mixture was inferior and erratic. This behavior can be ascribed to the presence of the crystalline form of the drug and the heterogeneity of the physical mixture. In consequence, on the grounds of the highest apparent solubility and excellent dissolution, formulation VI was selected as the optimal formulation in this study.

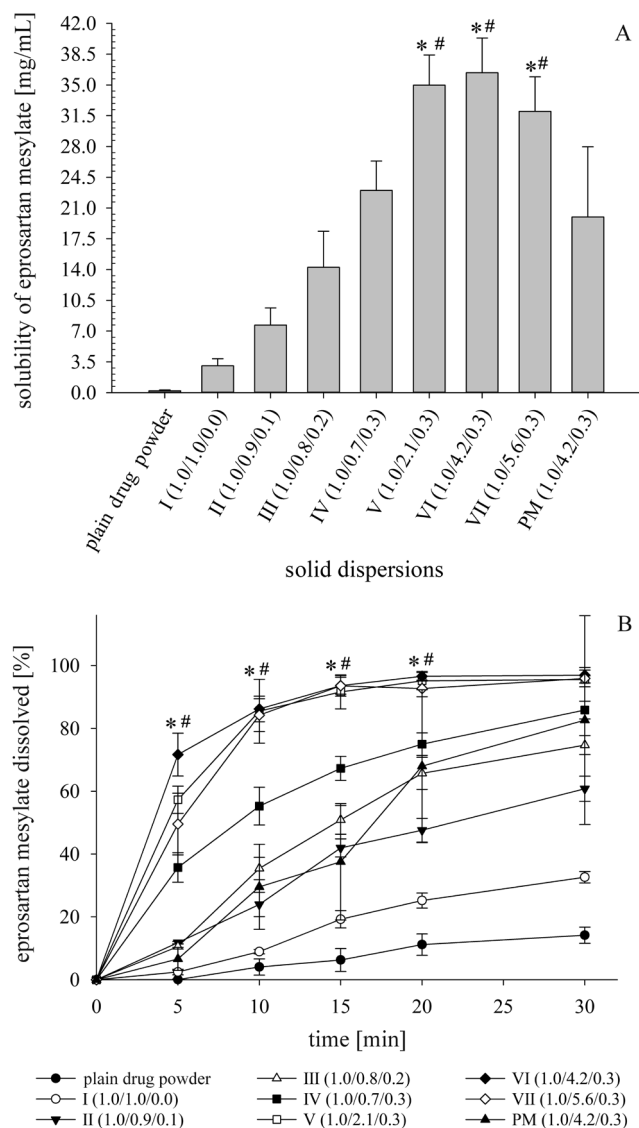


Fig. 2. The effect of polysorbate 80 (I–IV) and HPMC (V–VII) on the aqueous solubility (A) and dissolution (B) of eprosartan mesylate in solid dispersions; the solubility and dissolution of the drug in a physical mixture (PM) is also shown. Each value denotes the mean \pm SD of 3 solubility trials and 6 dissolution trials

* $p < 0.05$ compared with the plain drug powder and formulations I–IV; # $p > 0.05$ compared with formulations V–VII.

The XRD pattern of eprosartan mesylate showed typical crystalline peaks (Fig. 3A). Hydroxypropyl methylcellulose was amorphous; no sharp crystalline peaks appeared (Fig. 3B). Eprosartan mesylate-related peaks were also observed in the pattern of the physical mixture (Fig. 3C). In contrast, eprosartan was converted into the amorphous state in solid dispersion formulation VI (Fig. 3D), as no sharp peaks were seen, unlike the pattern of the physical mixture.

Similarly, the DSC curve of eprosartan mesylate showed a deep endotherm at about 251°C at its melting point (Fig. 4A), confirming its typical crystalline nature. No sharp endotherm appeared in the thermogram of HPMC, due to its amorphousness (Fig. 4B). However, a broad endothermic slide was seen between 40°C and 175°C.

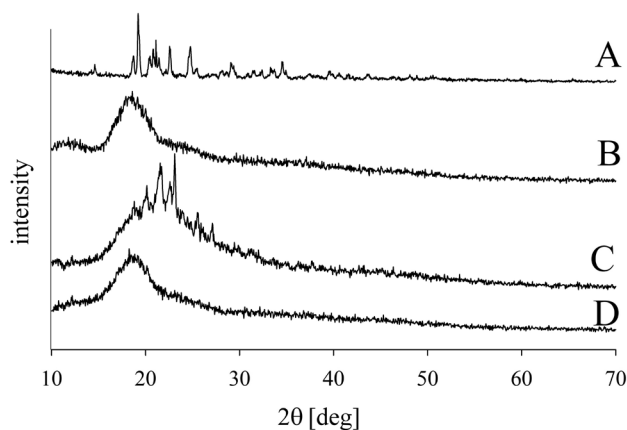


Fig. 3. X-ray diffraction (XRD) patterns: eprosartan mesylate (A), HPMC (B), the physical mixture (C), and solid dispersion VI (D)

An eprosartan-related endotherm was observed in the thermogram of the physical mixture (Fig. 4C); however, there was no endotherm in the thermogram of solid dispersion formulation VI (Fig. 4D). This confirmed that the drug was present in the crystalline state in the physical mixture, but was changed to the amorphous form in the solid dispersion. Thus, the DSC results were in harmony with the XRD patterns.

The shapes and surfaces of the particles of eprosartan mesylate (Fig. 5A), HPMC (Fig. 5B) and formulation VI (Fig. 5C) were observed by means of SEM. The plain eprosartan mesylate powder consisted of rod-shaped crystals with very rough surfaces. The particles of HPMC had irregular shapes and surfaces. The particles of formulation VI appeared as flakes.

In the FTIR spectrum, the chief distinctive peaks of eprosartan mesylate were at 743 cm^{-1} , 772 cm^{-1} , 830 cm^{-1} , 849 cm^{-1} , and 1154 cm^{-1} (Fig. 6A). These peaks were also clearly seen in the spectrum of the physical mixture (Fig. 6C). The spectrum of solid dispersion formulation VI (Fig. 6D) overlapped that of the physical mixture; the chief distinguishing peaks did not shift. This suggests that eprosartan mesylate has no strong bonding with the excipients.

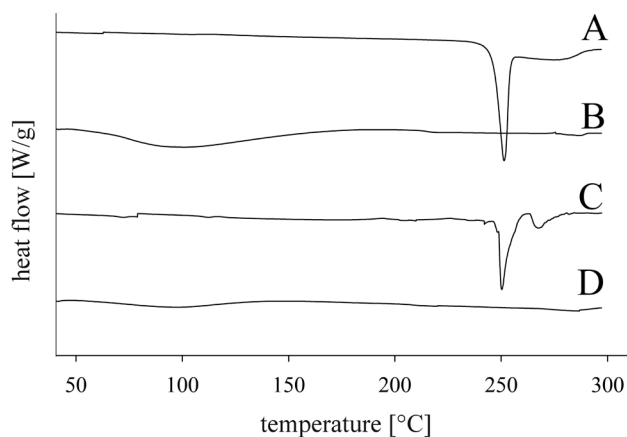


Fig. 4. Differential scanning calorimetry (DSC) thermograms: eprosartan mesylate (A), HPMC (B), the physical mixture (C), and solid dispersion VI (D)

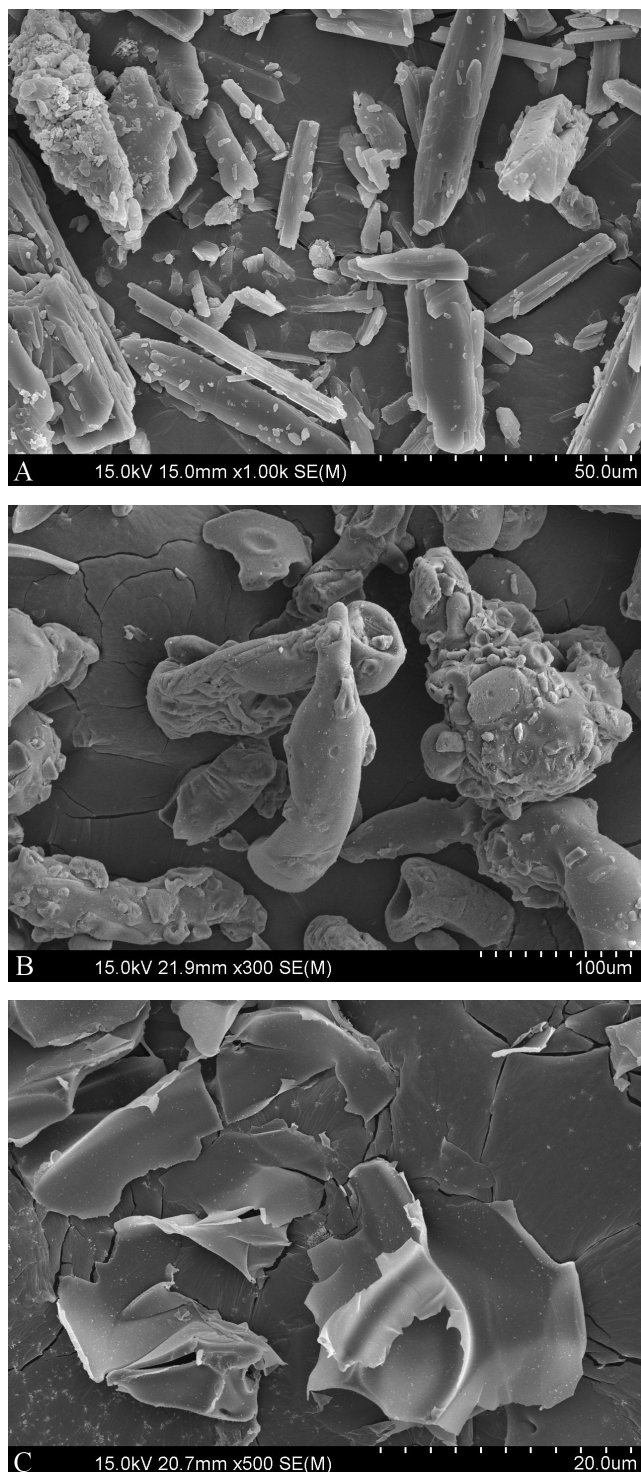


Fig. 5. Scanning electron microscopy (SEM) images: eprosartan mesylate ($\times 1000$) (A), HPMC ($\times 300$) (B) and solid dispersion VI ($\times 500$) (C)

Conclusions

Solid dispersion formulation VI, containing eprosartan mesylate, HPMC and polysorbate 80 at a ratio of 1.0/4.2/0.3 (w/w/w), showed the highest solubility (36.39 ± 3.95 mg/mL) and dissolution ($86.19 \pm 4.09\%$ in 10 min) among all the samples tested. The solubility was approx. 170 times higher than the solubility of the plain drug powder (36.39 ± 3.95 vs

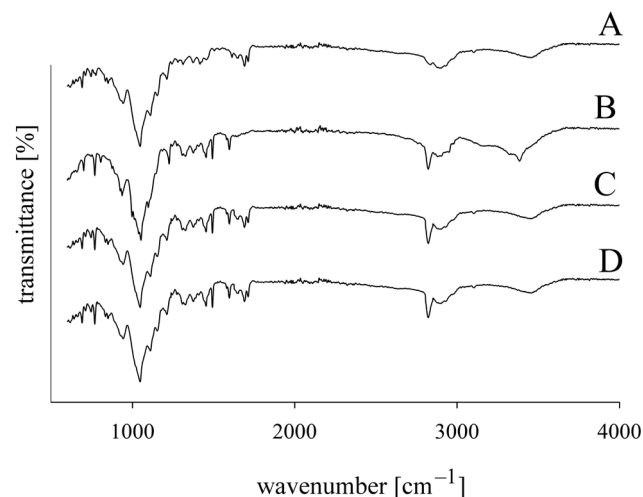


Fig. 6. Fourier-transform infrared spectroscopy (FTIR) spectra: eprosartan mesylate (A), HPMC (B), the physical mixture (C), and solid dispersion VI (D)

0.21 ± 0.10 $\mu\text{g/mL}$, respectively). Moreover, eprosartan mesylate was in the amorphous state in solid dispersion formulation VI, as shown by XRD and confirmed by DSC. Also, no covalent bonding existed between the drug and the excipients, as shown by the FTIR spectra. The particles of the formulation had irregular shapes and surfaces, and appeared as flakes. In view of the above, this formulation might be an effective system for the oral delivery of eprosartan mesylate with improved solubility and dissolution.

ORCID iDs

Abid Mehmood Yousaf <https://orcid.org/0000-0001-7866-9474>
 Sundas Zulfiqar <https://orcid.org/0000-0001-7579-7307>
 Yasser Shahzad <https://orcid.org/0000-0002-0974-2954>
 Talib Hussain <https://orcid.org/0000-0002-0465-9713>
 Tariq Mahmood <https://orcid.org/0000-0001-7097-5442>
 Muhammad Jamshaid <https://orcid.org/0000-0003-2682-7121>

References

- Vijaya Santhi D, Reddy NH, Sumalatha N, Jothieswari D. A novel estimation of eprosartan mesylate in pure and in tablet formulations by simple UV method. *Res J Pharm Technol.* 2011;4(7):1069–1072.
- Satheesh B, Pulluru SK, Nitin K, Saravanan D. Simultaneous determination of eprosartan, hydrochlorothiazide, and their related compounds in pharmaceutical dosage forms by UPLC. *J Liq Chromatogr Relat Technol.* 2011;34(17):1885–1900.
- Israili Z. Clinical pharmacokinetics of angiotensin II (AT1) receptor blockers in hypertension. *J Hum Hypertens.* 2000;14(S1):S73–S86.
- Hedner T, Himmelmann A; the Eprosartan Multinational Study Group. The efficacy and tolerance of one or two daily doses of eprosartan in essential hypertension. *J Hypertens.* 1999;17(1):129–136.
- McClellan KJ, Balfour JA. Eprosartan. *Drugs.* 1998;55(5):713–718, discussion 719–720.
- Sareen S, Mathew G, Joseph L. Improvement in solubility of poor water-soluble drugs by solid dispersion. *Int J Pharm Investig.* 2012;2(1):12–17.
- Derosa G, Ragonesi P, Mugellini A, Ciccarelli L, Fogari R. Effects of telmisartan compared with eprosartan on blood pressure control, glucose metabolism and lipid profile in hypertensive, type 2 diabetic patients: A randomized, double-blind, placebo-controlled 12-month study. *Hypertens Res.* 2004;27(7):457–464.
- Dézi CA. The different therapeutic choices with ARBs. Which one to give? When? Why? *Am J Cardiovasc Drugs.* 2016;16(4):255–266.

9. Joe JH, Lee WM, Park YJ, et al. Effect of the solid-dispersion method on the solubility and crystalline property of tacrolimus. *Int J Pharm.* 2010;395(1):161–166.
10. Yan YD, Sung JH, Kim KK, et al. Novel valsartan-loaded solid dispersion with enhanced bioavailability and no crystalline changes. *Int J Pharm.* 2012;422(1–2):202–210.
11. Cho JH, Kim YI, Kim DW, et al. Development of novel fast-dissolving tacrolimus solid dispersion-loaded prolonged release tablet. *Eur J Pharm Sci.* 2014;54(Suppl C):1–7.
12. Dave RH, Patel HH, Donahue E, Patel AD. To evaluate the change in release from solid dispersion using sodium lauryl sulfate and model drug sulfathiazole. *Drug Dev Ind Pharm.* 2013;39(10):1562–1572.
13. Hwang du H, Kim YI, Cho KH, et al. A novel solid dispersion system for natural product-loaded medicine: Silymarin-loaded solid dispersion with enhanced oral bioavailability and hepatoprotective activity. *J Microencapsul.* 2014;31(7):619–626.
14. Leane MM, Sinclair W, Qian F, et al. Formulation and process design for a solid dosage form containing a spray-dried amorphous dispersion of ibipinabant. *Pharm Dev Technol.* 2013;18(2):359–366.
15. Yousaf AM, Kim DW, Kim JO, et al. Characterization of physicochemical properties of spray-dried solid dispersions loaded with unmodified crystalline fenofibrate. *Curr Pharm Anal.* 2015;11(2):139–144.
16. Shahzad Y, Sohail S, Arshad MS, Hussain T, Shah SNH. Development of solid dispersions of artemisinin for transdermal delivery. *Int J Pharm.* 2013;457(1):197–205.
17. Yousaf AM, Mustapha O, Kim DW, et al. Novel electrosprayed nanospheres for enhanced aqueous solubility and oral bioavailability of poorly water-soluble fenofibrate. *Int J Nanomedicine.* 2016;11:213–221.
18. Yousaf AM, Kim DW, Kim DS, et al. Influence of polyvinylpyrrolidone quantity on the solubility, crystallinity and oral bioavailability of fenofibrate in solvent-evaporated microspheres. *J Microencapsul.* 2016;33(4):365–371.
19. Yousaf AM, Kim DW, Oh YK, Yong CS, Kim JO, Choi HG. Enhanced oral bioavailability of fenofibrate using polymeric nanoparticulated systems: Physicochemical characterization and in vivo investigation. *Int J Nanomedicine.* 2015;10:1819–1930.
20. Vasconcelos T, Sarmiento B, Costa P. Solid dispersions as strategy to improve oral bioavailability of poor water soluble drugs. *Drug Discov Today.* 2007;12(23):1068–1075.
21. Ming-Thau S, Ching-Min Y, Sokoloski TD. Characterization and dissolution of fenofibrate solid dispersion systems. *Int J Pharm.* 1994;103(2):137–146.
22. Modi A, Tayade P. Enhancement of dissolution profile by solid dispersion (kneading) technique. *AAPS PharmSciTech.* 2006;7(3):E87–92.
23. Patel T, Patel L, Patel T, Makwana S, Patel T. Enhancement of dissolution of fenofibrate by solid dispersion technique. *Int J Res Pharm Sci.* 2010;1(2):127–132.
24. Craig DQ. The mechanisms of drug release from solid dispersions in water-soluble polymers. *Int J Pharm.* 2002;231(2):131–144.
25. Shah V, Konecny J, Everett R, McCullough B, Noorizadeh AC, Skelly J. In vitro dissolution profile of water-insoluble drug dosage forms in the presence of surfactants. *Pharm Res.* 1989;6(7):612–618.
26. Shah VP, Noory A, Noory C, et al. In vitro dissolution of sparingly water-soluble drug dosage forms. *Int J Pharm.* 1995;125(1):99–106.
27. Hugo M, Kunath K, Dressman J. Selection of excipient, solvent and packaging to optimize the performance of spray-dried formulations: Case example fenofibrate. *Drug Dev Ind Pharm.* 2013;39(2):402–412.
28. Taylor LS, Zografi G. Spectroscopic characterization of interactions between PVP and indomethacin in amorphous molecular dispersions. *Pharm Res.* 1997;14(12):1691–1698.
29. Doherty C, York P. Accelerated stability of an X-ray amorphous frusemide-polyvinylpyrrolidone solid dispersion. *Drug Dev Ind Pharm.* 1989;15(12):1969–1987.
30. Konno H, Handa T, Alonzo DE, Taylor LS. Effect of polymer type on the dissolution profile of amorphous solid dispersions containing felodipine. *Eur J Pharm Biopharm.* 2008;70(2):493–499.
31. Gupta P, Kakumanu VK, Bansal AK. Stability and solubility of celecoxib-PVP amorphous dispersions: A molecular perspective. *Pharm Res.* 2004;21(10):1762–1769.
32. Tanno F, Nishiyama Y, Kokubo H, Obara S. Evaluation of hypromellose acetate succinate (HPMCAS) as a carrier in solid dispersions. *Drug Dev Ind Pharm.* 2004;30(1):9–17.
33. Dangre PV, Godbole MD, Ingale PV, Mahapatra DK. Improved dissolution and bioavailability of eprosartan mesylate formulated as solid dispersions using conventional methods. *Ind J Pharm Edu Res.* 2016;50(3):S209–217.
34. Ahn JS, Kim KM, Ko CY, Kang JS. Absorption enhancer and polymer (vitamin E TPGS and PVP K29) by solid dispersion improve dissolution and bioavailability of eprosartan mesylate. *Bull Korean Chem Soc.* 2011;32(5):1587–1592.

The polymorphism of statins and its effect on their physicochemical properties

Marta Karaźniewicz-Łada^{A-F}, Karina Bąba^{B-D}, Filip Dolatowski^{B-D}, Alicja Dobrowolska^{B-D}, Marlena Rakicka^{B-D}

Department of Physical Pharmacy and Pharmacokinetics, Poznan University of Medical Sciences, Poland

A – research concept and design; B – collection and/or assembly of data; C – data analysis and interpretation;
D – writing the article; E – critical revision of the article; F – final approval of the article

Polymers in Medicine, ISSN 0370-0747 (print), ISSN 2451-2699 (online)

Polim Med. 2018;48(2):77–82

Address for correspondence

Marta Karaźniewicz-Łada
E-mail: mkaraz@ump.edu.pl

Funding sources

The review was supported by the Polish National Science Centre (grant No. 2014/15/B/NZ7/00869).

Conflict of interest

None declared

Received on September 24, 2018

Reviewed on December 5, 2018

Accepted on January 16, 2019

Abstract

Polymorphism of pharmaceutical substances has a significant impact on their physicochemical properties, durability, bioavailability and consequently on their pharmacological activity. Solid dosage forms may exist in both crystalline and amorphous forms. Amorphous varieties are characterized by higher solubility and dissolution rates, while crystalline forms show greater purity and storage stability. The choice between the crystalline or amorphous form of a drug is extremely important to ensure effective and safe pharmacotherapy. Statins — the most commonly used group of drugs in the treatment of lipid disorders — are an example of drugs that occur in many crystalline and amorphous forms. Statins belong to class II in the biopharmaceutical classification system (BCS), which means that they are poorly soluble, but permeate biological membranes well. The bioavailability of statins shows considerable variation, which is associated with the first-pass effect in the liver and the accumulation of the drug in the hepatocytes. The improvement of bioavailability after oral administration of poorly soluble medicinal substances remains one of the most challenging aspects of the drug development process. A specific polymorphic form is obtained by applying appropriate conditions during the process of its preparation under industrial conditions, including the use of a suitable solvent, a specific temperature or rate of crystallization. The article provides a comprehensive update on the current knowledge of the influence of polymorphic form on statin solubility and bioavailability. Research is still being carried out to obtain new polymorphic varieties of statins that are characterized by better physicochemical and pharmacokinetic parameters.

Key words: bioavailability, solubility, amorphous substances, crystalline forms, statins

Cite as

Karaźniewicz-Łada M, Bąba K, Dolatowski F, Dobrowolska A, Rakicka M. The polymorphism of statins and its effect on their physicochemical properties. *Polim Med.* 2018;48(2):77–82. doi:10.17219/pim/102978

DOI

10.17219/pim/102978

Copyright

© 2019 by Wrocław Medical University

This is an article distributed under the terms of the Creative Commons Attribution Non-Commercial License (<http://creativecommons.org/licenses/by-nc-nd/4.0/>)

Introduction

Polymorphism is the occurrence of different crystalline forms of the same chemical substance. These forms differ in the geometry of a single cell that repeats in the 3 dimensions of the crystal. There are many medicinal substances that exhibit polymorphism. The same drug substance may exist in several polymorphic forms, depending on the distribution of molecules in the crystal lattice, which means individual variants may differ in their properties and activities. Therapeutic substances may also exist in amorphous forms, in which there is no regularity in the distribution of the structural elements and the molecules are arranged chaotically, like in liquids.^{1,2}

Individual polymorphic forms of the same drug substance may differ in their physical properties such as chemical reactivity, solubility and dissolution rate, stability, melting and sublimation temperature, density, hardness, adsorption, hygroscopicity and refractive index.^{1,2} Crystalline forms are thermodynamically more stable than amorphous varieties, which are high energy systems with a high free enthalpy. Amorphous substances demonstrate a tendency toward crystallization, which is a transition to an energy-beneficial system. The solubility and dissolution rate of crystalline forms are less than those of amorphous materials. The crystallites are also less hygroscopic. The better solubility of amorphous varieties results in their higher bioavailability, which is the fraction of the administered dose of the drug that gets into systemic circulation at a specific rate, and is a factor determining the pharmacological activity of the drug.³

The polymorphism of medicinal substances can be crucial in the production of a drug in the form of tablets under industrial conditions. Amorphous forms create problems at the formulation stage: they mix less and have worse rheological properties than crystalline systems.⁴ Among crystalline varieties, the most readily formulated into tablets are those with a symmetrical structure (e.g., tetragonal or regular), while substances that crystallize in the monoclinic system cause problems during tablet formulation.

The literature contains several examples of drugs that can occur in crystalline as well as in amorphous forms, including indomethacin,⁵ paracetamol,⁶ phenobarbital and nifedipine.⁷ Moreover, there are many poorly soluble drugs for which differences in polymorphic form solubility are crucial in terms of drug bioavailability, e.g., chloramphenicol palmitate, oxytetracycline, carbamazepine, ritonavir, phenylbutazone and rifaximin.⁸

Statins are the most commonly used group of drugs in the treatment of lipid disorders.⁹ They are inhibitors of 3-hydroxy-3-methylglutarylcoenzyme A (HMG-CoA) reductase, which is involved in the conversion of HMG-CoA to mevalonate, the primary substrate in the synthesis of cholesterol. Inhibition of this enzyme leads to a reduction in total cholesterol, low-density lipoprotein

(LDL) cholesterol and triglyceride (TG), and increases the concentration of high-density lipoprotein (HDL) cholesterol.¹⁰ Moreover, statins have various pleiotropic effects resulting from cholesterol-independent mechanisms of action, statins' ability to affect several tissue functions and the modulation of specific signal transduction pathways. The beneficial effects of statins include anti-inflammatory and antioxidant activity, improvement of endothelial function, increased bioavailability of nitric oxide and inhibition of the progression of atherosclerotic plaques.¹¹ Statins are classified into 3 categories based on their increasing potency and efficacy in lowering plasma LDL concentrations. First-generation statins included lovastatin, pravastatin and fluvastatin. Simvastatin and atorvastatin belong to the second generation, and rosuvastatin and pitavastatin to the third generation of statins.¹²

Many clinical studies have shown that from 13% to 75% of patients fail to achieve their target levels of LDL-cholesterol and total cholesterol.^{13,14} The underlying causes of statin resistance are multifactorial. It appears that both medication-specific and patient-specific factors contribute to the variability of cholesterol-lowering activity. The effectiveness of therapy with statins differs among compounds and may be decreased as a result of variability in the pharmacokinetics of this group of drugs. This variability may be caused by the different lipophilic properties of statins and their solubility. Statins belong to class II of the biopharmaceutical classification system (BCS), which means that they are poorly soluble, but they permeate biological membranes well. For low-solubility BCS II drugs, various oral formulation technologies, including salt formation, particle-size reduction, the use of lipid vehicles and co-solvents in the form of liquid-filled capsules, complexation, and more recently amorphous solid dispersions are designed to maximize the availability of the active pharmaceutical ingredient (API) in the gastrointestinal tract. Statins are an example of drugs that exist in an amorphous state and many crystalline forms, differing in their physical properties and pharmacological activity. Therefore, the polymorphic form of certain statins may significantly impact their bioavailability and in consequence their cholesterol-lowering effects.

In the current article, a comprehensive review of the available evidence regarding the effects of polymorphic form on statins' solubility and bioavailability is presented, including the possible clinical implications.

Polymorphism of statins

Atorvastatin

Atorvastatin is one of the most widely prescribed drugs in the world, and the most widely prescribed statin.¹⁵ It is the most effective statin in lowering cholesterol in LDL, non-HDL and other lipoproteins.¹⁶ Atorv-

astatin is usually marketed as its calcium trihydrate salt, which allows it to be conveniently formulated in pharmaceutical formulations. Like other statins, atorvastatin belongs to BCS class II. Its molecules have a lipophilic character; it is insoluble in aqueous solutions at $\text{pH} \leq 4$, and very slightly soluble in water and phosphate buffer at $\text{pH} 7.4$.¹⁷ However, atorvastatin penetrates the intestinal membrane very easily at the intestinal $\text{pH} 6\text{--}6.5$, and it absorbs into the blood quickly, achieving maximal concentration (C_{max}) after 1–2 h. About 30% of the administered dosage is absorbed in this way. However, due to the first-pass effect in the liver and intestine, and elimination by the mucous membrane of the stomach and intestine before reaching systemic circulation, the absolute bioavailability of atorvastatin is 14%.¹⁸ The bioavailability of the drug is one of the key parameters for many therapeutic indications. It is dependent on the form of the atorvastatin in the pharmaceutical formulation. More than 70 polymorphic forms of atorvastatin are known, among which crystalline forms are the majority, and at least 2 forms are amorphous (referred as “form 23” and “form 27”).¹⁹ The crystalline forms of atorvastatin have strictly defined properties; their solubility depends on the structure of the crystal network and the size of the molecules. These forms are more permanent in the thermodynamic sense than the amorphous forms; their solubility and dissolution rates are lower, which leads to lower bioactivity. On the other hand, atorvastatin in amorphous form has significantly more specific surface area, more substantial capacity to absorb solvents and is more reactive than the crystalline forms, which results in better solubility and bioavailability.¹⁷ Several techniques are commonly used for the transformation of the crystalline drug to the amorphous state, including supercritical anti-solvent precipitation and the spray drying process.^{20–22}

Numerous authors have characterized polymorphic forms of atorvastatin based on crystallographic and spectroscopic techniques. Shete et al. performed solid-state characterizations of commercial crystalline and amorphous atorvastatin samples available in the Indian market using X-ray powder diffractometry (XRPD), differential scanning calorimetry (DSC), thermogravimetric analysis, Karl Fisher titrimetry, microscopy, contact angle, and intrinsic dissolution rate (IDR).²³ The authors found that all the crystalline samples were stable form I, which had previously been characterized.²⁴ Amongst the amorphous atorvastatin samples, XRPD demonstrated that 5 samples were amorphous “form 27”, while one matched amorphous “form 23”.²⁵ The samples of amorphous atorvastatin had higher wettability and IDR than the crystalline samples, which may impact the performance and stability of the dosage form.²³ Kim et al. prepared amorphous atorvastatin hemi-calcium using the spray-drying and supercritical antisolvent (SAS) processes and compared its physicochemical properties

and oral bioavailability with the crystalline form after administration of both forms in 25 mg/kg doses to male rats.^{20,21} The oral absorption of amorphous atorvastatin calcium nanoparticles was higher compared with crystalline atorvastatin calcium, which was reflected by greater AUC and C_{max} values. The $\text{AUC}_{0\text{--}12\text{ h}}$ of the amorphous atorvastatin was 2.1 times that of the crystalline form.²¹ The enhancement in oral bioavailability of amorphous atorvastatin was attributed to a combination of higher apparent solubility and a higher dissolution rate due to its amorphous nature.

Rosuvastatin

Rosuvastatin is more effective at reducing LDL and TG levels in the blood plasma than statins of the first generation, including lovastatin or pravastatin, and its activity is 7 times greater than atorvastatin.²⁶ In contrast to atorvastatin, a molecule of rosuvastatin has a hydrophilic character, which determines the different pharmacokinetic properties of the drug in the body. After oral administration of rosuvastatin, C_{max} is obtained after 3–4 h, and the absolute bioavailability amounts to about 20%.²⁷ Rosuvastatin is converted to a slight degree (about 10%) into water-soluble derivative by the CYP2C9 isoenzyme, and its half-life amounts to about 19 h. In pharmaceuticals, rosuvastatin occurs in the form of a monohydrate calcium salt. At least 4 crystalline forms of rosuvastatin (A, B, B-1 and C) and 1 amorphous form are known. Form A is a pure crystalline compound; forms B and C are hydrated crystallines; and form B-1 is a dehydrated compound. When comparing the physicochemical properties of the crystalline forms, it was reported that forms B and C are much more soluble in water than form A and that this property may increase their bioavailability. Moreover, they are more thermostable than the amorphous form, which is less resistant to temperature changes, and in consequence less stable during the formulation process.^{28,29} The amorphous form of rosuvastatin is manufactured by the spray-drying and freeze-drying processes.³⁰ It is present in the medication called Crestor®.

Simvastatin

Simvastatin, along with atorvastatin and rosuvastatin, is one of the most commonly used statins in Poland.³¹ It is very well absorbed after oral administration (>90%) with C_{max} obtained after 1–2 h. Its bioavailability is very low (<5%), which is associated with the extensive metabolism of simvastatin by the isoenzyme CYP3A4.²⁷ Currently at least 3 crystalline³² and 2 amorphous forms of simvastatin are known.³³ When comparing the amorphous forms, it was found that they significantly differ in the size of molecules, physicochemical properties and stability. These differences come from distinct methods in the produc-

tion process of amorphous forms, including cryo-milling (CM) and melting and quench-cooling (QC). Zhang et al. reported that the solubility of the amorphous forms prepared by these 2 methods was enhanced compared to the crystalline form, and that the QC form was more soluble than the CM form.³⁴ In terms of physical stability, a higher crystallization rate was observed for the CM form, while the QC form exhibited lower molecular mobility and higher chemical degradation.³⁴

The superiority of amorphous simvastatin over the crystalline forms was confirmed by Singh et al.³⁵ The authors prepared an amorphous form of simvastatin by the process of fused dispersion. They observed an improvement in the dissolution rate at pH 6.8, with a maximum release of 99% of the amorphous drug in comparison to 21% release of the crystalline form. Moreover, the pharmacodynamic effect after the administration of both forms to rats with induced hypercholesterolemia was compared. Rats treated with amorphous simvastatin presented a 2.5-fold decrease in total cholesterol, a 1.5-fold increase in TG, a 1.4-fold decrease in LDL, a 2.4-fold decrease in VLDL, and a 1.3-fold increase in HDL-cholesterol compared to the rats treated with the crystalline form. These effects could be attributed primarily to the improved solubility and dissolution associated with the amorphization of the drug.³⁵

Pitavastatin

The potency of pitavastatin is dose-dependent and appears to be equivalent to that of atorvastatin. Pitavastatin is well absorbed from the gastrointestinal tract (>80%) and achieves C_{\max} about 1–2 h after administration. The absolute bioavailability of the drug is relatively high (about 60%).²⁷ It is available in pharmaceuticals in the form of sodium, calcium and magnesium salts. Several polymorphic forms of pitavastatin (designated as A, B, C, D, E, F and K) are known, as well as amorphous varieties. In the manufacturing process, the final crystalline form of pitavastatin is affected by the conditions of the crystallization process, which can be accelerated by adding the appropriate form of crystals in an amount not exceeding 5%.³⁶ Form K, compared to the other crystalline varieties, is characterized by better physical and chemical stability, which is extremely important in pre-formulation processes such as drying, grinding or granulation. There was no conversion of this form to another crystalline variety during the manufacturing or storage of the drug.³⁷ To obtain amorphous pitavastatin, concentrated solutions of the crystalline form in organic solvents, including 1,4-dioxane, tetrahydrofuran and ethyl methyl ketone, are exposed to non-solvents such as heptane or methyl-*t*-butyl ether. Lyophilization of an aqueous solution of pitavastatin calcium is also performed.³⁶ There is no data available on the differences between crystalline and amorphous forms in vivo conditions.

Fluvastatin

Fluvastatin has about 33% of the efficacy of atorvastatin in lowering cholesterol in LDL, non-HDL and remnant lipoproteins.¹⁶ Fluvastatin attains C_{\max} about 1–2 h after oral administration, and its bioavailability is 20–30%.²⁵ In pharmaceutical formulations, it occurs as the crystalline sodium salt in the form of a racemic mixture of the (3R, 5S) and (3S, 5R) enantiomers. Numerous crystalline forms (designated as A, B, C, D, E, F, JE, JF1, JF2 and JF3) and amorphous forms are currently distinguished. Individual forms differ from each other in terms of physicochemical properties. Form B is characterized by a lower hygroscopicity than form A and the amorphous form, which improves the handling and storage of the compound.^{38,39}

Pravastatin

Pravastatin, similarly to rosuvastatin, is a hydrophilic compound and it is metabolized to a small extent by cytochrome P450 enzymes. It is quickly absorbed from the gastrointestinal tract, obtaining C_{\max} after about 1 h, and its bioavailability is about 18%.²⁷ In pharmaceutical formulations, it is present as the crystalline form of the sodium salt. At present, at least 12 crystalline pravastatin varieties (known as A, B, C, D, E, F, G, H, I, J, K and L) are known to have similar physicochemical properties.⁴⁰ Chun et al. described a method for obtaining an amorphous form of the drug: they prepared crystalline pravastatin sodium solid dispersions using various bile salts and observed the complete conversion of the crystalline form into an amorphous form.⁴¹ The permeation flux of amorphous pravastatin from the solid dispersion was much higher than that of the crystalline form from physical mixtures and commercial tablets,⁴¹ which may improve the bioavailability of the compound in pharmaceutical formulations.

Lovastatin

Lovastatin is a crystalline powder that is practically insoluble in water (0.4 mg/mL); it has a partition coefficient (logP) of 4.26. Lovastatin is absorbed from the gastrointestinal tract (30%) and C_{\max} is attained after 2–4 h. As a result of the first-pass effect in the liver, the absolute bioavailability of the drug is only 5%.²⁷ Lovastatin does not show classic polymorphism. However, it is possible to distinguish crystals characterized by identical dimensions of elemental cells but with a different orientation. It has been found that depending on the crystallization conditions, 2 differing morphologically crystalline forms can be obtained, having the form of either plates or needles. This type of polymorphism does not have a significant effect on the physicochemical properties of the drug. Both forms have the same melting point, similar stability, solubility and reactivity. Yoshida et al. reported that

the preservative excipient butylhydroxyanisole causes amorphization of lovastatin crystallites and that the compound is therefore incompatible with lovastatin.⁴² Patel and Patel observed a decrease in the crystalline fraction of lovastatin and an increase in the amorphous fraction in solid dispersions of the drug prepared using polyethylene glycol 4000 and polyvinylpyrrolidone K30.⁴³ Lovastatin prepared in both polymers showed a better dissolution profile than that of the pure crystalline form.

Conclusions

Due to the differences between the crystalline and amorphous forms of drug substances, which affect not only their solubility and dissolution rates but also their storage stability, the choice of the appropriate form is extremely important to ensure effective and safe pharmacotherapy. It is particularly crucial for statins, which are poorly soluble and have low bioavailability. The low total bioavailability of statins creates the need for new polymorphic forms that will increase the therapeutic effect and reduce the dose of the drug taken by the patient. Based on the available scientific reports, it can be concluded that amorphous forms of statins create the possibility of increasing the solubility and bioavailability of this group of drugs, which in turn is an opportunity to increase their effectiveness in the treatment of cardiovascular diseases.

ORCID iDs

Marta Karaźniewicz-Łada  <https://orcid.org/0000-0003-4091-7035>

References

- Sykuła A, Łodyga-Chruścińska E, Zakrzewski M. *Impact of Polymorphism on Pharmaceutical Substances* [in Polish]. 2006. <http://repozytorium.p.lodz.pl/handle/11652/230>. Accessed June 14, 2018.
- Stańczak A, Stańczak C. Polimorfizm substancji farmaceutycznych. *Lek w Polsce*. 2013;23:50–58. <http://m.lekwpolsce.pl/download.php?dokid=52a06a0ef11fb>. Accessed October 31, 2018.
- Omar M, Makary P, Włodarski M. A Review of polymorphism and the amorphous state in the formulation strategy of medicines and marketed drugs. *UK J Pharm Biosci*. 2015;3(6):60. doi:10.20510/ukjpb/3/i6/87837
- Lu J, Rohani S. Polymorphism and crystallization of active pharmaceutical ingredients (APIs). *Curr Med Chem*. 2009;16(7):884–905.
- Kasten G, Nouri K, Grohgan H, Rades T, Lobmann K. Performance comparison between crystalline and co-amorphous salts of indomethacin-lysine. *Int J Pharm*. 2017;533:138–144. doi.org/10.1016/j.ijpharm.2017.09.063
- Sibik J, Sargent MJ, Franklin M, Zeitler JA. Crystallization and phase changes in paracetamol from the amorphous solid to the liquid phase. *Mol Pharm*. 2014;11(4):1326–1334. doi: 10.1021/mp400768m.
- Aso Y, Yoshioka S, Kojima S. Explanation of the crystallization rate of amorphous nifedipine and phenobarbital from their molecular mobility as measured by ¹³C nuclear magnetic resonance relaxation time and the relaxation time obtained from the heating rate dependence of the glass transition temperature. *J Pharm Sci*. 2001;90(6):798–806.
- Censi R, Di Martino P. Polymorph impact on the bioavailability and stability of poorly soluble drugs. *Molecules*. 2015;20(10):18759–18776. doi:10.3390/molecules201018759.
- Ramkumar S, Raghunath A, Raghunath S. Statin therapy: Review of safety and potential side effects. *Acta Cardiol Sin*. 2016;32:631–639.
- Istvan ES, Deisenhofer J. Structural mechanism for statin inhibition of HMG-CoA reductase. *Science*. 2001;292(5519):1160–1164. doi:10.1126/science.1059344
- Wang C-Y, Liu P-Y, Liao JK. Pleiotropic effects of statin therapy. *Trends Mol Med*. 2008;14(1):37–44. doi:10.1016/j.molmed.2007.11.004
- Maji D, Shaikh S, Solanki D, Gaurav K. Safety of statins. *Indian J Endocrinol Metab*. 2013;17(4):636–646. doi:10.4103/2230-8210.113754
- Shepherd J, Blauw GJ, Murphy MB, et al. Pravastatin in elderly individuals at risk of vascular disease (PROSPER): A randomised controlled trial. *Lancet Lond Engl*. 2002;360(9346):1623–1630.
- Reiner Ž, Tedeschi-Reiner E. Prevalence and types of persistent dyslipidemia in patients treated with statins. *Croat Med J*. 2013;54(4):339–345.
- Adams SP, Tsang M, Wright JM. Lipid-lowering efficacy of statin. *Cochrane Database Syst. Rev*. 2015;12:CD008226.
- Schaefer EJ, McNamara JR, Tayler T, et al. Comparisons of effects of statins (atorvastatin, fluvastatin, lovastatin, pravastatin, and simvastatin) on fasting and postprandial lipoproteins in patients with coronary heart disease versus control subjects. *Am J Cardiol*. 2004;93(1):31–39.
- Maurya D, Belgamwar V, Tekade A. Microwave induced solubility enhancement of poorly water soluble atorvastatin calcium. *J Pharm Pharmacol*. 2010;62(11):1599–1606. doi:10.1111/j.2042-7158.2010.01187.x
- Lennerhä H. Clinical pharmacokinetics of atorvastatin. *Clin Pharmacokinetic*. 2003;42(13):1141–1160. doi:10.2165/00003088-200342130-00005
- Discovering new crystalline fo- Titel- Elektronische Hochschulschriften. <http://digital.bibliothek.uni-halle.de/id/1390128>. Accessed June 14, 2018.
- Kim J-S, Kim M-S, Park HJ, Jin S-J, Lee S, Hwang S-J. Physicochemical properties and oral bioavailability of amorphous atorvastatin hemi-calcium using spray-drying and SAS process. *Int J Pharm*. 2008;359(1–2):211–219. doi:10.1016/j.ijpharm.2008.04.006
- Kim M-S, Jin S-J, Kim J-S, et al. Preparation, characterization and in vivo evaluation of amorphous atorvastatin calcium nanoparticles using supercritical antisolvent (SAS) process. *Eur J Pharm Biopharm*. 2008;69(2):454–465. doi:10.1016/j.ejpb.2008.01.007
- Zhang H-X, Wang J-X, Zhang Z-B, Le Y, Shen Z-G, Chen J-F. Micronization of atorvastatin calcium by antisolvent precipitation process. *Int J Pharm*. 2009;374(1–2):106–113. doi:10.1016/j.ijpharm.2009.02.015
- Shete G, Puri V, Kumar L, Bansal AK. Solid state characterization of commercial crystalline and amorphous atorvastatin calcium samples. *AAPS PharmSciTech*. 2010;11(2):598–609. doi:10.1208/s12249-010-9419-7
- Briggs CA, Jennings RA, Wade R, et al. Crystalline [R- (R*,R*)]-2-(4-Difluorophenyl)-β,δ-dihydroxy-5-(1-methylethyl)-3-phenyl-4-[(phenylamino)carbonyl]-1H-pyrrole-1-heptanoic acid hemi calcium salt (atorvastatin). October 1999. <https://patents.google.com/patent/US5969156A/en/und>. Accessed July 17, 2018.
- Zallen R. *The Physics of Amorphous Solids*. John Wiley & Sons; 2008.
- Luvai A, Mbagaya W, Hall AS, Barth JH. Rosuvastatin: A review of the pharmacology and clinical effectiveness in cardiovascular disease. *Clin Med Insights Cardiol*. 2012;6:17–33. doi:10.4137/CMC.S4324
- Karaźniewicz-Łada M, Glowka A, Mikołajewski J, Przysławski J. *Genetic and Non-Genetic Determinants of the Pharmacological Activity of Statins*. <http://www.ingentaconnect.com/contentone/ben/cdm/2016/00000017/00000009/art00006>. Published November 2016. Accessed July 17, 2018.
- Blatter F, Schaaf PAVD, Szelagiewicz M. Crystalline forms of rosuvastatin calcium salt. April 2011. <https://patents.google.com/patent/US7932387B2/en>. Accessed July 17, 2018.
- Wizel S, Niddam-Hildesheim V, Shabat S. Crystalline rosuvastatin calcium. March 2008. <https://patents.google.com/patent/WO2008036286A1/en>. Accessed July 17, 2018.
- Kumar Y, Rafeeq M, De S, Sathyanarayana S. Process for the preparation of amorphous rosuvastatin calcium. August 2007. <https://patents.google.com/patent/US20070191318A1/en>. Accessed July 17, 2018.
- Woźakowska-Kapłon B. Terapia hipercholesterolemii w schorzeniach układu sercowo-naczyniowego – jaki cel, jaka statyna, jaka dawka? *Folia Cardiol*. 2014;9(1):55–66.
- Tan NY, Zeitler JA. Probing phase transitions in simvastatin with terahertz time-domain spectroscopy. *Mol Pharm*. 2015;12(3):810–815. doi:10.1021/mp500649q

33. Graeser KA, Strachan CJ, Patterson JE, Gordon KC, Rades T. Physicochemical properties and stability of two differently prepared amorphous forms of simvastatin. *Cryst Growth Des.* 2008;8(1):128–135. doi:10.1021/cg700913m
34. Zhang F, Aaltonen J, Tian F, Saville DJ, Rades T. Influence of particle size and preparation methods on the physical and chemical stability of amorphous simvastatin. *Eur J Pharm Biopharm.* 2009;71(1):64–70. doi:10.1016/j.ejpb.2008.07.010
35. Singh H, Philip B, Pathak K. Preparation, characterization and pharmacodynamic evaluation of fused dispersions of simvastatin using PEO-PPO block copolymer. *Iran J Pharm Res IJPR.* 2012;11(2):433–445.
36. Schaaf PAVD, Blatter F, Szelagiewicz M, Schoening K-U. Crystalline forms of pitavastatin calcium. December 2014. <https://patents.google.com/patent/US20140364614A1/en>. Accessed July 18, 2018.
37. Kljajic A, Trost S, Pecavar A, Zupet R. Polymorphic form of pitavastatin calcium. July 2014. <https://patents.google.com/patent/EP2751081A1/en>. Accessed July 18, 2018.
38. Van DSPA, Marcolli C, Szelagiewicz M, Burkhard A, Wolleb H, Wolleb A. Crystalline forms of fluvastatin sodium. February 2003. <https://patents.google.com/patent/WO2003013512A2/en>. Accessed July 18, 2018.
39. Chavhan B, Awasthi AK, Aggarwal R, et al. Polymorphic forms of fluvastatin sodium and process for preparing the same. September 2010. <https://patents.google.com/patent/US7795451/en>. Accessed July 18, 2018.
40. Keri V, Szabo C, Aryai E, Aronhime J. Novel forms of pravastatin sodium. December 2005. <https://patents.google.com/patent/US20050288370/en>. Accessed July 18, 2018.
41. Chun IK, Lee KM, Lee KE, Gwak HS. Effects of bile salts on gastrointestinal absorption of pravastatin. *J Pharm Sci.* 2012;101(7):2281–2287. doi:10.1002/jps.23123
42. Yoshida MI, Oliveira MA, Gomes ECL, Mussel WN, Castro WV, Soares CDV. Thermal characterization of lovastatin in pharmaceutical formulations. *J Therm Anal Calorim.* 2011;106(3):657–664. doi:10.1007/s10973-011-1510-0
43. Patel RP, Patel MM. Physicochemical characterization and dissolution study of solid dispersions of lovastatin with polyethylene glycol 4000 and polyvinylpyrrolidone K30. *Pharm Dev Technol.* 2007;12(1):21–33. doi:10.1080/10837450601166510

Study of the influence of cellulose derivatives on physical and analytical attributes of a drug product belonging to BCS class II

Magdalena Domosławska^{A–F}, Renata Pawlak-Morka^{E,F}, Łukasz Dobrzyński^{E,F}, Monika Herda^B

Gedeon Richter Sp. z o.o., Research and Development Department, Grodzisk Mazowiecki, Poland

A – research concept and design; B – collection and/or assembly of data; C – data analysis and interpretation; D – writing the article; E – critical revision of the article; F – final approval of the article

Polymers in Medicine, ISSN 0370-0747 (print), ISSN 2451-2699 (online)

Polim Med. 2018;48(2):83–90

Address for correspondence

Magdalena Domosławska

E-mail: magda.domoslawska@gmail.com

Funding sources

None declared

Conflict of interest

None declared

Received on November 22, 2018

Reviewed on February 7, 2019

Accepted on February 17, 2019

Cite as

Domosławska M, Pawlak-Morka R, Dobrzyński Ł, Herda M. Study of the influence of cellulose derivatives on physical and analytical attributes of a drug product belonging to BCS class II. *Polim Med.* 2018;48(2):83–90. doi:10.17219/pim/104462

DOI

10.17219/pim/104462

Copyright

© 2019 by Wrocław Medical University

This is an article distributed under the terms of the Creative Commons Attribution 3.0 Unported (CC BY 3.0) (<https://creativecommons.org/licenses/by/3.0/>)

Abstract

Background. Cellulose microcrystalline (MCC), hydroxypropyl methylcellulose (HPMC) and croscarmellose sodium are cellulose derivatives which are widely used in pharmaceutical technology. Although they are inert pharmaceutical ingredients, they can influence the release profile of an active substance from the dosage form depending on their distribution, type and quantity used in the formulation.

Objectives. The aim of the present investigation was to examine the effect of chosen cellulose derivatives on the physical and analytical attributes of a drug product containing an active substance of Biopharmaceutics Classification System (BCS) class II.

Material and methods. The tablets were prepared using the wet granulation technology. The batches differed in the amount and grade of HPMC, the type of MCC and the distribution of croscarmellose sodium. The granule properties as well as physical (tablet hardness, disintegration time, friability) and analytical (dissolution profile in different media) attributes of the tablets were examined.

Results. The flow characteristics were satisfying in the case of all prepared batches. However, the differences in flow properties were visible, especially in the cases where MCC of coarser particles was replaced with MCC of finer particles. The type of MCC used in the product formula also had a significant influence on the drug product dissolution profile. The batches in which MCC of finer particles was used had substantially better results, regardless of HPMC viscosity type and the distribution of croscarmellose sodium between the inner and outer phase. What is more, the differences in the results between batches of different MCC types were especially visible in dissolution conditions, i.e., 0.1N hydrochloric acid (HCl).

Conclusions. By choosing the right type, quantity and distribution of cellulose derivatives, it was possible to obtain the optimal formula of the drug product similar to in-vitro conditions to the reference drug. Out of all the tested excipients, the type of cellulose microcrystalline was found to have the most critical influence on both physical and analytical properties of the pharmaceutical formulation.

Key words: wet granulation, dissolution profile, cellulose derivatives, drug formulation technology

Introduction

Cellulose is one of the most commonly used polymers in pharmaceutical technology. It is a high-molecular-weight linear biopolymer consisting of D-glucose units joined by β -(1,4) linkages. It is a biodegradable, low-cost, renewable, and easily accessible material with high bio-compatibility, which makes its use so common in various fields.¹

In pharmaceutical technology, there are several cellulose derivatives which play a different role in the product formulation, i.e., tablet filler (cellulose microcrystalline – MCC), binder (ether derivatives: hydroxypropyl methylcellulose – HPMC, hydroxypropylcellulose, methylcellulose, ethylcellulose), superdisintegrant (croscarmellose sodium), and film-coating agent (the above-mentioned ether derivatives). They can also be used to create modified-release drug products as well as osmotic and bioadhesive delivery systems. What is more, cellulose derivatives are gaining more and more popularity in nanotechnology due to the possibility of obtaining compounds such as nanofibrillar cellulose and cellulose nanocrystal.^{1–4}

Cellulose microcrystalline is a purified, partially depolymerized cellulose. It is a white, crystalline powder with porous particles. It is commercially available in several grades which have different properties and applications.⁵ Hydroxypropyl methylcellulose, also known as hypromellose, is a partly *O*-methylated and *O*-(2-hydroxypropylated) cellulose. It is commercially available in different grades that vary in viscosity properties and the extent of substitution. Hypromellose is usually used as binder in the wet granulation process in concentrations up to 5% w/w.^{5,6} Croscarmellose sodium is a cross-linked polymer of carboxymethylcellulose sodium. It belongs to the superdisintegrant group, i.e., the substances which facilitate fast disintegration and can be used in a smaller quantity than disintegrants, usually up to 5% w/w in the case of tablets.^{4,5}

The above-mentioned cellulose derivatives were used during the development of a generic drug product with an active substance of Biopharmaceutics Classification System (BCS) class II. The influence of the said excipients (their type, grade, amount per tablet, and/or distribution in the tablet) on the physical and analytical attributes of the product was examined. The reference drug is considered as very rapidly dissolving, i.e., at least 85% of the labeled amount of the drug substances is dissolved within 15 min.⁷ The developed generic product has to fulfill the same dissolution criteria. The qualitative composition of the prepared batches is similar to the composition of the reference product. In both cases, the MCC, HPMC and croscarmellose sodium polymers were used.

The BCS is a scientific framework which helps to classify active substances regarding their solubility and permeability. The active substance which was used in the study belongs to BCS class II. This means that it shows low water solubility and high permeability. In recent years, the number of the newly developed drugs which have poor

solubility properties has significantly increased. It has been stated that among new drug candidates, almost 70% show poor water solubility. When the active substance has solubility limitations, its bioavailability can be significantly affected, even if the substance is highly permeable. Therefore, the solubility of the active substance is a very important physical property, and thus in vitro dissolution testing can play a key role in drug development.^{8–10}

Material and methods

Material

The following materials were used: active substance of BCS class II, lactose monohydrate, MCC PH200, MCC PH101, croscarmellose sodium, HPMC 6cP, HPMC 3cP, sodium lauryl sulfate, and magnesium stearate. All substances used in the study were purchased from external suppliers.

Methods

Pre-formulation studies

During the pre-formulation studies, the Raman spectrum was performed for the active substance used in the study and the reference product in order to check that the same polymorphic form of the active substance as in the reference product was used. The parameters of powder X-ray diffraction measurements were as follows: instrument – PANalytical X'Pert PRO MPD; radiation: CuK α , voltage: 40 kV, anode current: 40 mA, goniometer: PW3050/60, scan rate: 0.0305°/s, step size: 0.0131°, sample holder: PW181/25&40 (transmission, sample between foils), sample spinner: PW3064/60 (reflection/transmission spinner), sample spin rate: 1 rpm, detector: PIXcel (PW3018/00).

What is more, the particle size measurement of the active substance was performed using the Mastersizer 2000 particle size analyzer.

Preparation of tablets via high-shear granulation process

The active substance, lactose monohydrate, MCC, croscarmellose sodium, and hypromellose were put into a high-shear mixer. The granulating fluid was prepared by dispersing HPMC in water and, in the next step, the addition and dissolution of sodium lauryl sulfate. After mixing the dry powders, the granulation fluid was added into the high-shear mixer and the granulation step was performed. The wet granules were sieved and dried in a fluid-bed dryer. The dried granules were sieved, and the outer phase was added and mixed. The final granules were compressed into tablets using the Riva Piccola laboratory rotary tablet press machine with 8 punch sets fitted in the tablet press turret. The compression force used

during the tableting process was in the range between 4 and 6 kN. The rotation speed was 15 rpm. The obtained tablets had a diameter of 5.5 mm.

Preparation of tablets via fluid-bed granulation process

The active substance, lactose monohydrate, MCC, croscarmellose sodium and hypromellose were put into a fluid-bed granulator. The granulating fluid was prepared by dispersing HPMC in water and, in the next step, the addition and dissolution of sodium lauryl sulfate. After mixing the dry powders, the granulation fluid was added into the fluid-bed granulator, and the granulation and drying step were performed. The dried granules were sieved, and the outer phase was added and mixed. The final granules were compressed into tablets using the Riva Piccola laboratory rotary tablet press machine with 8 punch sets fitted in the tablet press turret. The compression force used during the tableting process was in the range between 4 and 6 kN. The rotation speed was 15 rpm. The obtained tablets had a diameter of 5.5 mm.

Determination of bulk density and tapped density

The final granulate was taken into a 250-milliliter measuring cylinder and the initial volume was recorded. The measuring cylinder was tapped the specified number of times using the ERWEKA tapped volumeter. The bulk density and tapped density were calculated according to the following formulas:

$$\text{bulk density} = \frac{\text{weight of the final granulate}}{\text{initial volume}} [\text{g/mL}] \quad (1)$$

$$\text{tapped density} = \frac{\text{weight of the final granulate}}{\text{final volume after tapping}} [\text{g/mL}] \quad (2)$$

Determination of Hausner ratio

The Hausner ratio was calculated based on the following formula:

$$\text{Hausner ratio} = \frac{\text{tapped density}}{\text{bulk density}} \quad (3)$$

Determination of Carr's compressibility index

The Carr's index was calculated based on the following formula:

$$\text{Carr's index} = \frac{\text{tapped density} - \text{bulk density}}{\text{bulk density}} \times 100 \quad (3)$$

Flowability

The flow properties of the final granules were determined using a granulate tester (ERWEKA GTB; ERWEKA). A minimum of 100 g of the granules were introduced into a dry funnel whose bottom opening had been blocked. In the next step, the bottom opening of the funnel was unblocked and the sample flowed out of the funnel. Flowability was determined as the time needed for the 100 g of the sample to flow out of the funnel and as the time needed for the 100 mL of the sample to flow out of the funnel. The diameter of the nozzle used in the analysis was 10 ± 0.01 mm.

Determination of particle size distribution

The degree of fineness of the final granulate was established using the Analysette 3 PRO vibratory sieve shaker. The assessment of the particle size distribution of the final granules was evaluated by allowing the material to pass through a series of sieves (100 μm , 180 μm , 250 μm , 355 μm , 500 μm , and 800 μm) and weighing the amount of granules that was stopped by each sieve as a fraction of the whole mass.

Tablet hardness

The tablet hardness was determined using the Multi-Check 3 tester (ERWEKA). The measurements were conducted on 10 tablets of each batch.

Friability test

The friability test was conducted using the TDR 100 ERWEKA friability tester (ERWEKA). In order to perform the test, a sample of minimum 6.5 g of tablets was weighted. Before weighing, any loose dust from the tablets was removed. After weighing, the tablets were placed into the drum. The drum was rotated 100 times. After that, the tablets were removed from the drum and weighted again in order to establish the weight loss.

Disintegration time

The disintegration time of the tablets was determined using the Pharma Test PTZ AUTO. The test was conducted on 6 tablets of each batch. In order to perform the test, 1 dosage unit was placed in each of the 6 tubes of the basket and a disc was added. The test was performed using water as medium at a temperature of $37 \pm 2^\circ\text{C}$. According to the current edition of the European Pharmacopoeia (Ph. Eur.), the tablets should disintegrate in less than 15 min.¹¹

Dissolution profile

In order to determine the dissolution profile of the tablets, a paddle apparatus (Apparatus II USP) and a UV-VIS spectrophotometer were used. The test was

conducted on 6 tablets of each batch and the results were compared to the results of the reference product. In order to establish similarity between the tested batches and the reference product, the following dissolution media were applied:

- 0.2% sodium dodecyl sulfate (SDS) in acetate buffer pH 4.5;
- 0.1N hydrochloric acid (HCl);
- acetate buffer pH 4.5;
- phosphate buffer pH 6.8.

The rest of the dissolution conditions were identical for each dissolution medium: dissolution apparatus – type II with paddle agitators; volume of dissolution medium: 500 mL; paddle speed: 75 rpm; temperature: $37 \pm 0.5^\circ\text{C}$; duration time: 60 min.

The volume of the dissolution medium was decreased from a standard value of 900 mL to 500 mL due to the low absorbance of the active substance. The European Pharmacopoeia allows using dissolution medium in volumes 500–1000 mL.¹¹

A dissolution profile analysis was conducted according to the following description: The tablets were added to each of the 6 apparatus vessels containing the dissolution medium heated to the prescribed temperature. The process was started with a rotation speed of 75 rpm. During the test, samples of the solution were taken at the following time points: 5 min, 10 min, 15 min, 20 min, 30 min, 45 min, 50 min, and 60 min. The samples were filtered through a 10-micrometer filter. Next, the absorbance value of the test solutions and a suitable standard solution were determined spectrophotometrically at a wavelength of 200–400 nm, using 10-millimeter cuvettes, against the dissolution medium as a blank.

The above-mentioned analysis is specific, i.e., the blank solution and the solution of all known impurities for the active substance do not show any absorbance at a wavelength characteristic for the active substance. What is more, the spectrum obtained for the test solution and the standard solution are similar and show the maxima of absorbance at the same wavelengths (± 2 nm).

The first sample during the analysis was collected after 5 min of testing. Although the disintegration time of the tablets is very short (<5 min), it does not mean that the active substance is already fully dissolved in the medium after the disintegration. The active substance releases from the surface of the tablet as well as from the tablet residue after the disintegration.

Results and discussion

Pre-formulation study

The active substance is a white crystalline powder, practically insoluble in water (<10 mg/L), in aqueous acidic medium (<10 mg/L in 0.1M HCl) or in higher pH

(<10 mg/L for pH 9.0). It is slightly soluble in organic solvents and its log P value is at the level of 1.5. The active substance has more than one polymorphic form. However, the polymorphic form used in the study was confirmed via the X-ray diffraction analysis to be the same as the one in the reference product.

The active substance in the reference product is in a micronized form. Therefore, the active substance used in the study underwent a micronization process as well. In order to check its particle size distribution, the active substance sample was measured via the laser diffraction method and the results show that $d(0.9)$, which corresponds to 90% of the cumulative undersize distribution, is <30 μm .

Formulation study

In order to obtain the most suitable formula which would be similar to the reference product, batches F1–F9 were produced. Batches F1–F4 differed in the amount of HPMC 6cP. Hydroxypropyl methylcellulose plays a binder role in the tablet formulation. In the case of batch F5, HPMC 6cP was replaced with HPMC of lower viscosity, i.e., 3cP. One batch – F6 – was produced using different manufacturing technology from the rest of the trials – the granulate was obtained via the fluid-bed granulation. Usually, it is possible to obtain finer granules using the wet granulation process via a fluid-bed granulator instead of a high-shear mixer. The aim of preparing batch F6 was to check if the manufacturing of significantly smaller granules would have an influence on the dissolution profile results. The qualitative as well as quantitative composition of batch F6 is exactly the same as for batch F5. What is more, the granulation fluid was identical and all the other steps of the process, except the granulation part, were kept the same. In the case of batches F7–F9, MCC PH200 which was used as a tablet filler was replaced with MCC of finer particles, i.e., PH101. More detailed information about the batch compositions are presented in Table 1.

Evaluation of granules

In order to characterize the powder flow of the prepared batches F1–F9, the following methods were used: flow rate through an orifice, angle of repose, the compressibility index, and the Hausner ratio (Table 2).

The flow rate of the granules was measured in 2 ways: as the time it takes for 100 g of the granules to pass through the orifice and as the time it takes for 100 mL of the granules to pass through the orifice. The best results (the shortest time) in the case of both methods were obtained for batch F4, which contains MCC of coarser particles (PH200) and HPMC of higher viscosity (6cP). The worst results (the longest time) were found for batch F7, where MCC of coarser particles was replaced with MCC of finer particles (PH101) and HPMC 6cP was replaced with HPMC 3cP.

Table 1. Composition of prepared batches F1–F9

Qualitative and quantitative composition of the prepared batches [%/tablet]										
Formulation code	F1	F2	F3	F4	F5	F6	F7	F8	F9	
Manufacturing technology	wet granulation via high-shear mixer				wet granulation via fluid-bed granulator			wet granulation via high-shear mixer		
Inner phase										
Active substance	≤12.5	≤12.5	≤12.5	≤12.5	≤12.5	≤12.5	≤12.5	≤12.5	≤12.5	
Lactose monohydrate	35.38	35.00	35.5	34.79	34.79	34.79	34.79	34.79	34.79	
MCC PH200	52.25	51.88	52.38	51.34	51.34	51.34	–	–	–	
MCC PH101	–	–	–	–	–	–	51.34	51.34	51.34	
Croscarmellose sodium	2.50	2.50	5.00	5.00	5.00	5.00	5.00	5.00	2.50	
HPMC 6cP	0.63	1.00	1.00	1.88	–	–	–	1.88	1.88	
HPMC 3cP	–	–	–	–	1.88	1.88	1.88	–	–	
Granulating fluid										
HPMC 6cP	0.63	1.00	1.00	1.88	–	–	–	1.88	1.88	
HPMC 3cP	–	–	–	–	1.88	1.88	1.88	–	–	
Sodium lauryl sulfate	2.00	2.00	1.00	1.00	1.00	1.00	1.00	1.00	1.00	
Water	27.00	27.00	27.00	27.00	27.00	27.00	27.00	27.00	27.00	
Outer phase										
Croscarmellose sodium	2.50	2.50	–	–	–	–	–	–	2.50	
Magnesium stearate	1.00	1.00	1.00	1.00	1.00	1.00	1.00	1.00	1.00	

MMC – cellulose microcrystalline; HPMC – hydroxypropyl methylcellulose

The angle of repose reflects the resistance to movement between the particles. According to European Pharmacopoeia (Ph. Eur.), when the angle of repose is above 50 degrees, the flow is rarely acceptable for manufacturing purposes.¹¹ In the case of all batches, the angle of repose was below 50 degrees. However, there is a significant difference in the results between the batches with MCC of coarser particles and the batches in which MCC PH200 was replaced with MCC PH101.

The next 2 methods used in order to evaluate the flow characteristics of the granules are compressibility index and the Hausner ratio. Both of the methods are determined by measuring the bulk and tapped volume of the final granules. According to the flowability scale (Ph. Eur.), results above 25% for the compressibility index and 1.34 for the Hausner ratio indicate poor flow properties.¹¹

The flow character for most of the prepared batches was determined as good (compressibility index: 11–15%, Hausner ratio: 1.12–1.18). The worst results were obtained for batch F8 (the flow character determined as passable) and the best results were obtained for batch F2 (the flow character determined as excellent).

The particle size distribution for all prepared batches was determined via the sieve analysis (Table 3). There is a significant difference between the granule particle size of the batches prepared using MCC PH200 and the batches where MCC PH200 was replaced with MCC PH101. Due to the fact that MCC is present in the composition of batches in high amounts, it is obvious that it has a significant influence on the particle size distribution of the final granules. In the case of batches F7–F9, approx. 50% of the particles are <100 µm, which means that the granules are

Table 2. Flow properties of granules

Batch number	Bulk density [g/mL]	Tapped density [g/mL]	Hausner ratio	Carr's compressibility index [%]	Flow rate [s/100 g]	Volume flow rate [s/100 mL]	Angle of repose
F1	0.53	0.60	1.14	12.0	36.5 ±0.97	18.2 ±0.10	39.5 ±1.17
F2	0.54	0.60	1.11	9.6	27.3 ±0.17	12.3 ±0.06	40.8 ±0.49
F3	0.5	0.56	1.13	11.2	27.8 ±0.32	11.9 ±0.12	39.3 ±0.38
F4	0.48	0.54	1.13	11.2	21.9 ±0.52	9.2 ±0.06	38.8 ±0.75
F5	0.49	0.55	1.13	11.2	24.7 ±6.27	18.4 ±3.82	38.2 ±1.65
F6	0.46	0.53	1.16	13.6	32.4 ±0.10	12.3 ±0.15	38.4 ±0.40
F7	0.52	0.63	1.21	17.6	49.1 ±12.54	14.7 ±0.46	45.6 ±0.95
F8	0.51	0.64	1.26	20.89	28.5 ±0.64	13.2 ±1.43	46.1 ±1.70
F9	0.53	0.65	1.21	17.6	46.0 ±2.50	17.1 ±2.29	43.1 ±1.95

Table 3. Particle size distribution of granules

Batch number	Sieve analysis of final granulate [%]						
	<100 μm	100–180 μm	180–250 μm	250–355 μm	355–500 μm	500–800 μm	>800 μm
F1	29.1	22.6	20.6	21.6	5.2	0.7	0.2
F2	21.6	22.4	21.1	23.5	9.6	1.6	0.2
F3	22.3	20.9	20.9	23.8	9.1	2.9	0.1
F4	16.4	16.4	18.3	26.8	17.0	4.8	0.2
F5	21.1	19.8	19.8	24.9	12.3	1.9	0.1
F6	31.7	32.1	21.3	13.7	1.0	0.2	0
F7	54.3	17.4	7.4	7.8	10.9	2.0	0.1
F8	51.8	14.8	5.9	8.2	14.3	4.9	0.1
F9	47.8	16.1	6.9	9.1	15.2	4.8	0.1

very fine. Batch F6, which was prepared via the fluid-bed granulation, is characterized by an intermediate particle size distribution, placing itself between batches F7–F9 and F2–F5. Very fine particles were also obtained in batch F1, in which HPMC 6cP was added at the lowest amount. Batches F2–F5 had the largest particle size and, according to Ph. Eur., are determined as moderate fine, i.e., the median size (X50) of the particles is in the range of 180–355 μm .¹¹

Evaluation of tablet cores

The following physical parameters of the tablet cores were determined: tablet hardness, disintegration time and tablet friability (Table 4). For all of the batches, the mean tablet hardness is in the range of 50–70 N. For all of the batches, the disintegration time is <15 min, which complies with the requirements for uncoated tablets.¹¹ The shortest disintegration time was observed in the case of batch F8 and the longest disintegration time was observed for batch F4. All batches present very satisfying friability test results. In all cases, the tablet friability is below or close to 0.1% w/w.

All batches underwent the dissolution profile analysis. The results obtained were compared to the results of the dissolution profile for the reference sample.

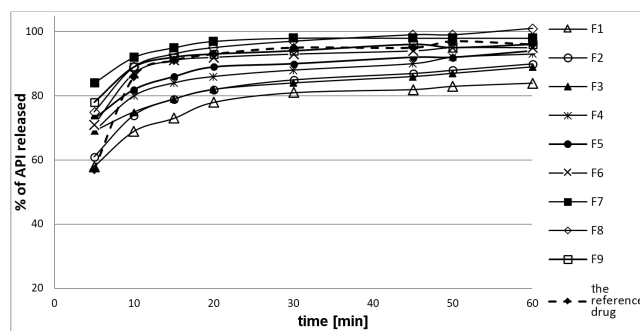
Table 4. Physical parameters of tablet cores (compression force during tableting – 6 kN)

Batch number	Hardness [N]	Disintegration time [min]		Friability [%]
		min–max	mean \pm SD	
F1	59 \pm 1.84	2:52–3:00	2:56 \pm 0:03	0.069
F2	58 \pm 1.35	3:24–3:50	3:37 \pm 0:10	0.037
F3	67 \pm 2.11	3:10–3:50	3:33 \pm 0:16	0.120
F4	71 \pm 2.46	3:50–4:30	4:10 \pm 0:16	0.054
F5	65 \pm 3.11	3:12–3:30	3:21 \pm 0:07	0.013
F6	60 \pm 4.11	3:38–3:56	3:50 \pm 0:07	0.006
F7	58 \pm 3.27	2:32–3:02	2:48 \pm 0:10	0.096
F8	68 \pm 2.99	1:54–2:18	2:06 \pm 0:10	0.019
F9	62 \pm 2.99	2:22–2:52	2:37 \pm 0:10	0.032

The results of the dissolution profile in chosen media for batches F1–F9 (Fig. 1) show that by increasing the amount of HPMC it was possible to obtain a faster drug release. What is more, the replacement of HPMC 6cP with HPMC of lower viscosity (3cP) resulted in slightly better results, more similar to the reference product. The effect of dissolution profile improvement was especially visible when the granulation method was changed from high-shear mixing to fluid-bed granulation. However, the best dissolution profile results were obtained when MCC of coarser particles was replaced with MCC of finer particles, regardless of the type of HPMC used and the distribution of croscarmellose sodium.

For rapidly dissolving products, 2 dissolution profiles can be considered as similar without further mathematical evaluation when >85% of the active substance dissolves within 15 min. The comparison of dissolution profile results in acetate buffer pH 4.5 with 0.2% SDS after 15 min of testing is provided in Table 5. Based on the results obtained, it can be stated that batches F6–F9 are similar to the reference product.

The level of similarity between the developed product and the reference drug should be as high as possible. One of the methods which can evaluate the level of similarity in in-vitro conditions is performing the dissolution profile analysis in 3 different media. Therefore, 3 different batches were chosen: F5, F6 and F9, and the analysis of the dissolution profile in the following dissolution media was performed: 0.1N HCl, acetate buffer pH 4.5 and

**Fig. 1.** Dissolution profile results for batches F1–F9 in acetate buffer pH 4.5 with 0.2% sodium dodecyl sulfate

phosphate buffer pH 6.8 (Fig. 2). The analysis carried out under acidic conditions (0.1N HCl) show significant differences between the tested batches. The worst results were obtained in the case of batch F5. Slightly better results were obtained for batch F6, which has the same qualitative and quantitative composition as batch F5, but it was produced with a different wet granulation technique, i.e., via the fluid-bed granulation. The results for batches F5–F6 are significantly lower than for batch F9 and the reference product. Out of all the batches tested, batch F9 seems to be the most similar to the reference drug.

Conclusions

It was found that cellulose derivatives presented in the composition of a drug product with an active substance of BCS class II had a significant influence on the physi-

cal and analytical attributes of the product. Out of all the prepared batches, the best results with regard to granule properties were obtained for batches MCC of coarser particles and HPMC of higher viscosity. However, the results of the dissolution profile for these batches differed significantly when compared to the results of the reference product. The dissolution profile enhanced when HPMC of higher viscosity was replaced with HPMC of lower viscosity (batch F5). What is more, the dissolution profile was even better when the granulation technology used in batch F5 was changed from high-shear mixing to fluid-bed granulation (batch F6) while using the same qualitative and quantitative composition. However, despite very promising dissolution profile results in 0.2% SDS in acetate buffer, which was established as the chosen dissolution medium, the analysis in 3 different media showed significant differences in acidic conditions, i.e., 0.1N HCl, between batch F6 and the reference product.

Table 5. Comparison of dissolution profile results in acetate buffer pH 4.5 with 0.2% sodium dodecyl sulfate (SDS) after 15 min of testing

Batch		Reference product	F1	F2	F3	F4	F5	F6	F7	F8	F9
average for 6 samples		90	73	79	79	70	86	91	95	93	92
% of API dissolved in 15 min	min	85	71	76	77	66	82	86	92	93	90
	max	93	78	82	82	74	90	96	97	94	93
	RSD [%]	3.6	5.5	3.9	2.5	4.4	3.6	4.7	2.5	0.6	1.1
Is the batch similar to the reference product?		–	no	no	no	no	yes/no*	yes	yes	yes	yes

API – active pharmaceutical ingredients; RSD – relative standard deviation; * The average is above 85%; however, some of the results are still below 85%.

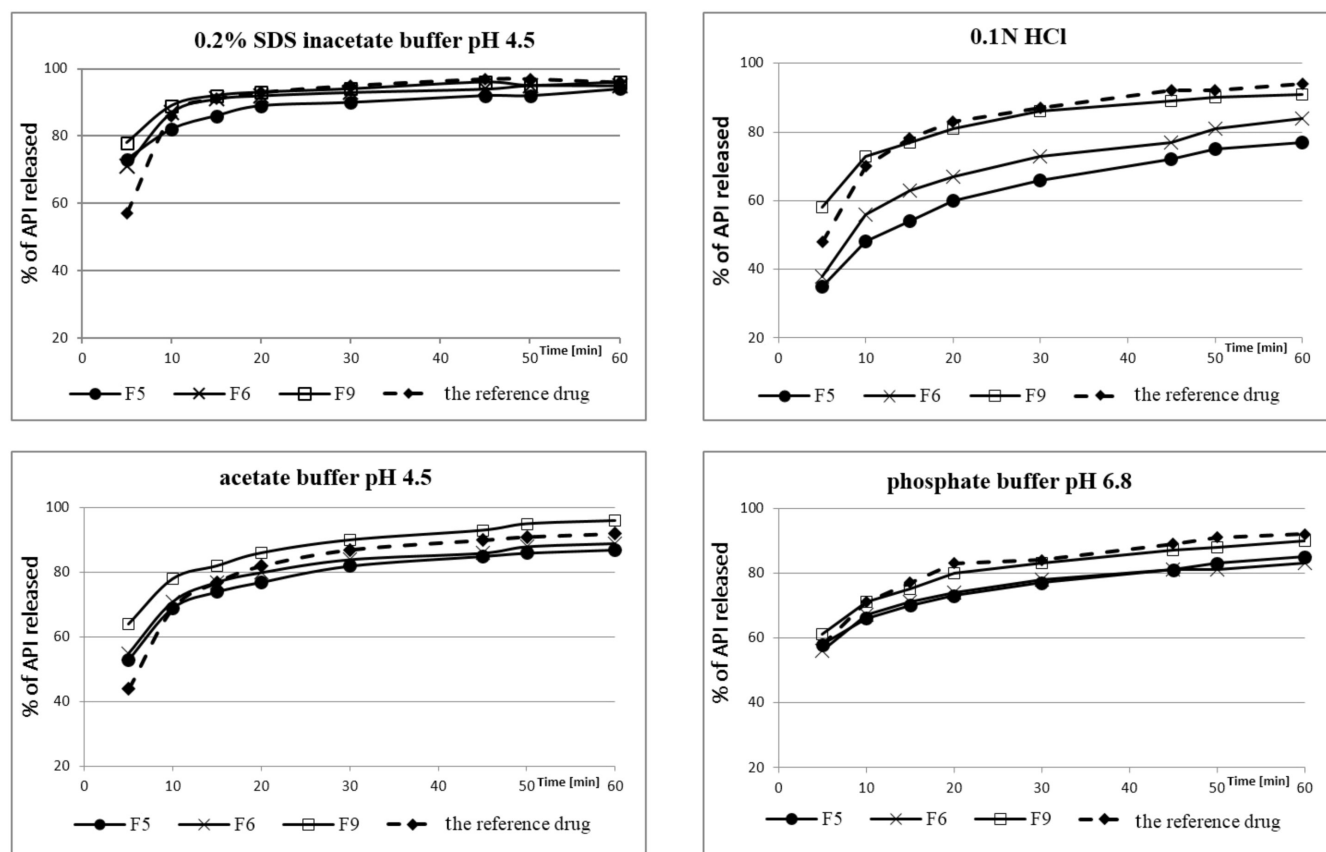




Fig. 2. Dissolution profile results in different media for chosen batches F5, F6 and F9 in comparison to the reference product


Therefore, further changes in the composition are required. The preparation of batches F7–F9 showed that the type of MCC used had the most critical influence on the dissolution profile out of all the cellulose derivatives tested. The dissolution profile in chosen media was similar in the case of all batches where MCC of coarser particles was replaced with MCC of finer particles, regardless of the HPMC viscosity type used and the distribution of croscarmellose sodium. The results of the dissolution profile in 3 different media for the chosen batch F9 showed very high similarity to the reference product.

ORCID iDs

Magdalena Domosławska  <https://orcid.org/0000-0002-4896-4648>

Renata Pawlak-Morka  <https://orcid.org/0000-0001-8828-6661>

Łukasz Dobrzyński  <https://orcid.org/0000-0002-6289-7242>

Monika Herda  <https://orcid.org/0000-0002-3825-1687>

References

1. Halib N, Perrone F, Cemazar M, et al. Potential applications of nanocellulose-containing materials in the biomedical field. *Materials*. 2017;10:977.
2. Shokri J, Adibkia K. Application of Cellulose and Cellulose Derivatives in Pharmaceutical Industries. In: Van De Ven TGM, ed. *Cellulose Medical, Pharmaceutical and Electronic Applications*. Intech; 2013.
3. Kubiak-Tomaszewska G, Tomaszewski P, Pachecka J. Hypromellose in pharmaceutical technology of capsules and other medicinal product dosage forms. *Pediatr Med Rodz*. 2011;7(3):271–276.
4. Rawat S, Derle DV, Fukte SR, Shinde PR, Parve BS. Superdisintegrants: An overview, *World J Pharm Pharm Sci*. 2014;3(5):263–278.
5. Rowe RC, Sheskey PJ, Quinn ME. *Handbook of Pharmaceutical Excipients*. 6th ed. London; 2009:129–133, 206–208.
6. Hamed E, Moe D, Khankari R, Hontz J. Binders and Solvents. In: Parikh DM, Raton B, ed. *Handbook of Pharmaceutical Granulation Technology*. 2nd ed. North Carolina, Pinehurs: PharmaceuTech Inc.; 2005:109–125.
7. US Department of Health and Human Services Food and Drug Administration Center for Drug Evaluation and Research. *Waiver of in Vivo Bioavailability and Bioequivalence Studies for Immediate-Release Solid Oral Dosage Forms Based on a Biopharmaceutics Classification System Guidance for industry*. US Department of Health and Human Services Food and Drug Administration Center for Drug Evaluation and Research; 2017.
8. Khadka P, Kim JRH, Kim I, et al. Pharmaceutical particle technologies: An approach to improve drug solubility, dissolution and bioavailability. *AJPS*. 2014;9(6)304–316.
9. US Department of Health and Human Services Food and Drug Administration Centre for Drug Evaluation and Research. *Guidance for Industry Dissolution Testing of Immediate Release Solid Oral Dosage Forms*. US Department of Health and Human Services Food and Drug Administration Centre for Drug Evaluation and Research; 1997.
10. International Council for Harmonisation of Technical Requirements for Pharmaceuticals for Human Use. *ICH Harmonised Guideline. Biopharmaceutics Classification System-Based Biowaivers M9* [draft version]. Geneva: International Council for Harmonisation of Technical Requirements for Pharmaceuticals for Human Use; 2018.
11. European Pharmacopoeia. 7th Edition. Vol. 1. <https://pl.scribd.com/document/367962556/European-Pharmacopoeia-7-0-Vol-1-pdf>

Effects of media components and agricultural by-products on γ -polyglutamic acid production by *Bacillus toyonensis* As8

Olubusola A. Odeniyi^{A–F}, David S. Avoseh^{B–F}

University of Ibadan, Nigeria

A – research concept and design; B – collection and/or assembly of data; C – data analysis and interpretation; D – writing the article; E – critical revision of the article; F – final approval of the article

Polymers in Medicine, ISSN 0370-0747 (print), ISSN 2451-2699 (online)

Polim Med. 2018;48(2):91–97

Address for correspondence

Olubusola A. Odeniyi
E-mail: busolaodeniyi@gmail.com

Funding sources

None declared

Conflict of interest

None declared

Received on August 31, 2018
Reviewed on February 4, 2019
Accepted on March 12, 2019

Cite as

Odeniyi OA, Avoseh DS. Effects of media components and agricultural by-products on γ -polyglutamic acid production by *Bacillus toyonensis* As8. *Polim Med.* 2018;48(2):91–97. doi:10.17219/pim/105555

DOI

10.17219/pim/105555

Copyright

© 2019 by Wrocław Medical University
This is an article distributed under the terms of the
Creative Commons Attribution 3.0 Unported (CC BY 3.0)
(<https://creativecommons.org/licenses/by/3.0/>)

Abstract

Background. Poly- γ -glutamic acid (γ -PGA) provides an environmentally friendly alternative to plastic materials which have widely polluted the environment.

Objectives. The microbial production of γ -PGA, an amino acid biopolymer with glutamic acid subunits, was investigated using renewable agricultural residues in an attempt to find cheaper substitutes for conventional synthetic media components.

Material and methods. Bacteria which produce γ -PGA were isolated through depolymerizing *Coix lacryma-jobi*, a cellulosic grass, and the effects of various carbon and nitrogen sources, temperature, inoculant load, incubation period, and pH on γ -PGA yield were determined after submerged fermentation. Bacterial growth was measured turbidimetrically at 550 nm. The γ -PGA produced was characterized using Fourier transform infrared (FT-IR) spectroscopy and the polymer shape was determined using scanning electron microscopy (SEM).

Results. The best γ -PGA producer was molecularly identified as *Bacillus toyonensis* As8. The conditions which produced the highest γ -PGA yield were glucose, ammonium sulfate, 25°C, a pH of 5.5, and an incubation period of 48 h. This bacterium yielded the most γ -PGA (26.45 g/L) on cassava peels, while other agro-wastes (corn cob, sorghum leaves, *Coix noir* leaves, and rice bran) also supported bacterial growth with lower γ -PGA yields than conventional carbon sources. The wrinkled γ -PGA had absorbance peaks of hydroxyl, amide, carbonyl, and amine groups comparable with the ranges of those found in commercial γ -PGA.

Conclusions. The use of agricultural by-products as fermentation substrates increased γ -PGA yield and may therefore be used as substitute components in γ -PGA production.

Key words: agricultural wastes, biopolymer synthesis, poly- γ -glutamic acid characteristics, *Bacillus toyonensis*

Introduction

Poly- γ -glutamic acid (γ -PGA) is a non-toxic, anionic, water-soluble, and biodegradable homopolyamide consisting of D- and L-glutamic acid units polymerized by γ -amide linkages and found between α -amino and γ -carboxylic acid groups^{1–3} (with the molecular formula $(C_5H_7NO_3)_n$). In light of the many undesirable properties associated with the use of chemically manufactured products, γ -PGA – along with many other biopolymers – has enjoyed a growing interest due to its biodegradability and non-toxicity. When compared with other production methods – such as chemical synthesis, peptide synthesis and biotransformation – microbial fermentation is considered the most cost-effective, having numerous advantages: minimal environmental pollution, potential production using inexpensive raw materials, high natural product purity, and mild reaction conditions.^{3–5} This important biopolymer has been found in species from all domains of life, including archaea, bacteria and eukaryotes.^{6,7} The traditional Japanese food natto – *Bacillus subtilis*-fermented soybeans – contains a naturally occurring mucilaginous mixture of γ -PGA and fructan. Apart from *Bacillus*, many other species have been reported to produce γ -PGA, such as *Planococcus*, *Sporosarcina*, *Staphylococcus*, *Fusobacterium*, *Natrialba*, and *Hydra*.^{3–7} At present, microbial fermentation of biomass is still the most preferred means of commercial γ -PGA production.⁵

The desirable properties of γ -PGA as a safe, biodegradable, edible, eco-friendly, and water-soluble biopolymer make it and its derivatives important as food thickeners, bitterness-relieving agents,⁸ humectants, cryoprotectants,⁹ sustained-release materials, drug delivery agents, biological adhesives, heavy metal absorbers, bioflocculants, dye-removing agents, fertilizer synergists, and biodegradable plastics. Other potential applications may include its use as a contrast agent or vaccine adjuvant, or in the areas of immobilization, microencapsulation, gene delivery, and tissue engineering.^{1,8–10}

Although the process leading to the microbial fermentative biosynthesis of γ -PGA is well-known, some challenges remain, such as the cost and suitability of substrate media for optimal yields, a fact which limits economically viable commercial applications. In addition to the important efforts currently directed at finding a lasting solution to various problems associated with γ -PGA production for commercial applications, there is a need to continue the search for potential γ -PGA producers with unique properties. In this study, the effects of media components and the suitability of agricultural byproducts as substrates for γ -PGA production in flask fermentation by various bacteria were investigated.

Material and methods

Sample collection, microorganisms and screening for γ -PGA production on a solid medium

The *Bacillus toyonensis* (*B. toyonensis*) As8 used in this experiment was isolated from samples of decomposing *Coix lacryma-jobi* collected from a fallow agricultural farm of the University of Ibadan, Nigeria. The bacteria were isolated through serial dilutions of the samples¹¹ inoculated using the pour plate method on nutrient agar and incubated at 30°C for 24 h. Bacterial colonies observed on the surface of the nutrient agar were picked at random, based on differences in colonial morphology, and were streaked onto the surface of nutrient agar to obtain distinct colonies representative of a single pure isolate.

Screening for γ -PGA production

Pure cultures of each bacterial isolate were cultivated on a solid medium composed of 1 g/L glucose, 0.5 g/L yeast extract, 1 g/L L-glutamic acid, 0.05 g/L KH_2PO_4 , 0.01 g/L $MgSO_4$, and 15 g/L agar (pH 7.0) at 37°C for 24 h.¹² Sticky, highly viscous colonies forming on the agar – examined for stickiness with gentle touches using a sterile inoculating needle – were considered γ -PGA-producing bacterial isolates. The isolates (10% v/v 24-hour-old broth culture, equivalent to 10⁸ CFU/mL) selected from the solid screening medium as described previously were grown at 37°C on a shaker incubator (ZHWHY211E, New Brunswick Scientific Company, New Jersey, US) at 150 rpm for 72 h in a conical flask containing 100 mL of screening broth (10 g/L L-glutamic acid, 10 g/L glucose, 5 g/L $(NH_4)_2SO_4$, 1 g/L K_2HPO_4 , 1 g/L KH_2PO_4 , 0.5 g/L $MgSO_4 \cdot 7H_2O$, 0.02 g/L $MnSO_4$, and 0.05 g/L $FeCl_3 \cdot 7H_2O$). After 72 h of incubation, the broth culture was centrifuged at 12,000 rpm for 20 min at 4°C to obtain cell-free supernatants, after which an equal volume of cold ethanol was added to the supernatant to yield a fibrous precipitate regarded as the crude γ -PGA. This precipitate was concentrated with centrifugation and was subsequently oven-dried at 55°C to a constant weight; the weight was then measured.^{12,13} The best γ -PGA-producing bacteria were identified with morphological, biochemical and 16S rRNA gene sequencing using universal primers.^{11,14,15}

Recovery and quantification of the produced γ -PGA

The cells were separated from the fermentation broth with 20 min of centrifugation at 12,000 rpm to obtain a cell-free supernatant. The γ -PGA was precipitated from the supernatant through the addition of 4 volumes of 95% ethanol with gentle stirring. The mixture was then stored

in a refrigerator (Haier THERMOCOOL BD-124E, HPZ Nigeria) at 4°C for 12 h. The resulting precipitate containing crude γ -PGA was collected using a high-speed refrigerated centrifuge (Hitachi Himae CR21GII, Hitachi Group, Tokyo, Japan) at 12,000 rpm for 20 min at 10°C. The crude γ -PGA was oven-dried at 55°C to a constant weight, which was then measured.⁶

Effects of medium components and environmental conditions on γ -PGA production

The effects of environmental conditions and the components of the medium on γ -PGA production using the selected bacterial isolates were investigated using the one-factor-at-a-time method with a PGA basal medium containing 5 g/L $(\text{NH}_4)_2\text{SO}_4$, 1 g/L K_2HPO_4 , 1 g/L KH_2PO_4 , 0.5 g/L $\text{MgSO}_4 \cdot 7\text{H}_2\text{O}$, 0.02 g/L MnSO_4 , and 0.05 g/L $\text{FeCl}_3 \cdot 7\text{H}_2\text{O}$.¹³ Variables such as the effects of different carbon sources (glucose, fructose, maltose, lactose, sucrose, citric acid, and starch) and nitrogen sources (peptone, urea, yeast extract, L-glutamic acid, ammonium sulfate, ammonium chloride, and sodium nitrate), pH (4.5 to 9.0 in 0.1M phosphate buffers), incubation temperature (25°C, 30°C, 35°C, 40°C, and 45°C), different inoculant loads (1% and 10%), and incubation period (24–96 h) on the production medium were investigated in order to determine the ones which are most conducive to γ -PGA production. To measure the effects of the different carbon sources, the basal medium contained 20 g/L L-glutamic acid, 10 g/L $(\text{NH}_4)_2\text{SO}_4$, 1 g/L K_2HPO_4 , 1 g/L KH_2PO_4 , 0.5 g/L $\text{MgSO}_4 \cdot 7\text{H}_2\text{O}$, 0.02 g/L MnSO_4 , and 0.05 g/L $\text{FeCl}_3 \cdot 7\text{H}_2\text{O}$. The L-glutamic acid was then substituted for each of the sugars listed above. Likewise, to test the effects of nitrogen sources, the basal medium contained 20 g/L glucose, 10 g/L $(\text{NH}_4)_2\text{SO}_4$, 1 g/L K_2HPO_4 , 1 g/L KH_2PO_4 , 0.5 g/L $\text{MgSO}_4 \cdot 7\text{H}_2\text{O}$, 0.02 g/L MnSO_4 , and 0.05 g/L $\text{FeCl}_3 \cdot 7\text{H}_2\text{O}$; $(\text{NH}_4)_2\text{SO}_4$ was then substituted for the other nitrogen sources.

To measure the effects of pH, incubation temperature and incubation period, the basal medium consisted of 20 g/L L-glutamic acid, 20 g/L glucose, 10 g/L $(\text{NH}_4)_2\text{SO}_4$, 1 g/L K_2HPO_4 , 1 g/L KH_2PO_4 , 0.5 g/L $\text{MgSO}_4 \cdot 7\text{H}_2\text{O}$, 0.02 g/L MnSO_4 , and 0.05 g/L $\text{FeCl}_3 \cdot 7\text{H}_2\text{O}$.¹³ A loopful of 18–24-hour-old nutrient agar culture of the γ -PGA-producing bacterium was transferred into the PGA broth and incubated at 35°C for 24 h. A 10% v/v dilution of this preparation was used as an inoculant for the experiments. The fermentation flasks were incubated with agitation at 150 rpm over 4 days. Bacterial growth was determined with optical density using a Jenway 6405 UV-VIS spectrophotometer (Cole-Parmer, UK) at 550 nm.^{6,16}

The effects of different agricultural wastes (corn cob, sorghum leaves, *Coix noir* leaves, cassava peel, and rice bran) as carbon sources for γ -PGA production by the selected γ -PGA producers were investigated. Freshly collected agricultural

wastes were oven-dried at 45°C, pulverized and sieved to obtain powder-sized particles. Each of these substrates (20 g/L) was added into the γ -PGA production medium as the major source of carbon and autoclaved at 121°C for 15 min, after which they were allowed to cool to room temperature and were inoculated as described previously. They were then incubated at 35°C on a shaker incubator (ZHWY211E, New Brunswick Scientific Company, New Jersey, US) at 150 rpm for 72 h. At the end of the incubation, the fermentation broth was diluted with an equal volume of sterile distilled water and centrifuged using the refrigerated centrifuge at 12,000 rpm for 20 min to recover the γ -PGA; the yield was then measured.^{6,16} The best environmental variables and agricultural wastes for the highest γ -PGA yield in these experiments were used to produce γ -PGA.

In all cases, the means of triplicate experimental readings were used.

Characteristics of γ -PGA

The peaks of the spectra of key functional groups in the γ -PGA produced in the experiments were identified using Fourier transform infrared (FT-IR) spectroscopy. Their absorption spectra, with peaks corresponding to specific bonds in the γ -PGA product, were compared with standards characteristic of amine (C–N), carbonyl (C=O), amide (N–H), and hydroxyl (OH) groups in the ranges of 1085–1165 cm^{-1} , 1394–1454 cm^{-1} , 1620–1655 cm^{-1} , and 3400–3450 cm^{-1} , respectively.^{17,18} Scanning electron microscopy (SEM) was also used to determine the surface morphology of the polymer produced. An FEI Inspect S50 scanning electron microscope (FEI Company, Japan) with an acceleration voltage of 10kV was used. The polymer samples were placed on a metallic stub and sputtered with gold film under vacuum; images were taken at different levels of magnification.

Results and discussion

Screening of isolates for γ -PGA production

Approximately 14% of the 36 isolates obtained from the decomposing *Coix lacryma-jobi* (As8, Is6, Is7, Is13, and Is14) produced viscous colonies when screened. The highest yield from the submerged fermentation, 16.53 g/L of γ -PGA, was recovered from the As8 fermentation culture. This was followed by isolates Is14, Is6, Is7, and Is13 with γ -PGA yields of 14.82 g/L, 14.07 g/L, 12.58 g/L, and 9.42 g/L, respectively. The 5 γ -PGA-positive isolates were Gram-positive, facultative, anaerobic spore formers and were presumptively identified as *Bacillus* species (Table 1). Phenotypic and biochemical techniques have been successfully used in the past to identify different microorganisms in microbiology.¹⁶ Isolate As8, the most prolific γ -PGA producer, was capable of metabolizing different

Table 1. Morphological and biochemical characteristics of poly- γ -glutamic-acid (γ -PGA)-producing bacteria

γ -PGA-producing isolates	As8	Is6	Is7	Is13	Is14
Gram's reaction	+	+	+	+	+
Morphology	short rods	rods	rods	rods	rods
Endospore staining	+	+	+	+	+
Gelatin hydrolysis	+	+	+	+	+
Starch hydrolysis	+	+	+	+	+
Proteolysis	+	+	+	+	+
Hemolysis	+	–	–	–	–
Lecithinase test	+	–	+	–	+
Catalase test	+	+	+	+	+
Citrate utilization	+	+	–	+	+
Methyl red test	–	–	–	–	–
Voges–Proskauer test	+	+	+	+	+
Glucose	+	–	+	–	+
Fructose	+	+/-	+	–	+
Lactose	–	–	–	+	+
Maltose	+	+/-	–	+/-	+
Sucrose	+	–	–	+	+
Galactose	–	–	+/-	–	+
Raffinose	–	+	–	–	+/-
Probable identity of the organism	<i>Bacillus</i> sp. As8	<i>Bacillus</i> sp. Is6	<i>Bacillus</i> sp. Is7	<i>Bacillus</i> sp. Is13	<i>Bacillus</i> sp. Is14

(+) – positive; (–) – negative; (+/–) – variable.

sugars (such as glucose, fructose and maltose) and tested positive for utilizing catalase, protease, lecithinase, and citrate, as well as for starch hydrolysis and gelatin hydrolysis. The isolate As8, however, did not metabolize lactose, galactose or raffinose. Genotypically, *Bacillus* sp. As8 was 96% percent similar to the *B. toyonensis* strain BCT-7112 and was therefore referred to as *B. toyonensis* As8.

Growth and γ -PGA production responses of *Bacillus toyonensis* As8 to physicochemical modifications of medium components

Bacillus toyonensis As8 (the representative colony depicted in Fig. 1A) had the highest γ -PGA yield (16.53 g/L) with glucose and fructose as carbon sources, while its yield in a starch-based medium was the lowest (4.06 g/L) – even though that substrate was highly conducive to bacterial growth (Fig. 1B). All of the sugars used as carbon sources supported bacterial growth. These findings may be attributed to the fact that simple sugars are more desirable for bacterial metabolism since less energy is required to incorporate them into the metabolism of a cell. However, Ju et al.¹⁹ obtained a higher γ -PGA yield with 30 g/L of starch in the fermentation medium and *B. subtilis* MJ80, yielding 48.3 g/L of γ -PGA. The findings that citric acid and starch supported bacterial growth may be attributed to the ease with which these compounds convert into glutamic acids, through the tricarboxylic acid cycle and finally into poly- γ -glutamate.²⁰

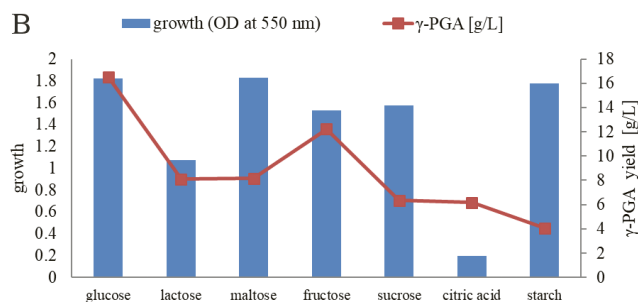
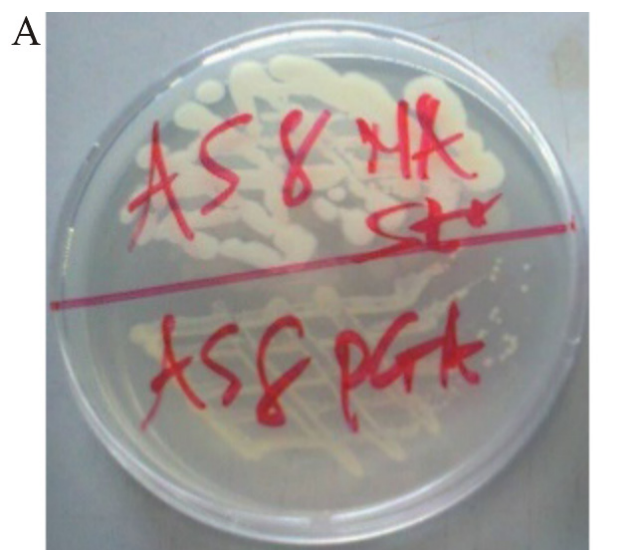


Fig. 1. (A) Colonial view of *Bacillus toyonensis* As8. (B) Effect of different carbon sources on the growth and poly- γ -glutamic-acid (γ -PGA) yield of *Bacillus toyonensis* As8

Ammonium sulfate supported both bacterial growth (optical density: 1.854) and γ -PGA production (19.95 g/L) by *B. toyonensis* As8 (Fig. 2). Organic peptone and malt extract did support γ -PGA production, though less so than inorganic ammonium sulfate. Because γ -PGA was produced in the medium containing ammonium sulfate in the absence of L-glutamic acid, we may deduce that *B. toyonensis* As8 can be classified as an L-glutamic acid-independent γ -PGA-producing strain.³

There was a progressive reduction in γ -PGA yield as the incubation temperature increased (Fig. 3), indicating that the γ -PGA yield from *B. toyonensis* As8 was temperature-dependent.¹⁶ Production was highest at 25°C, with a dry weight of 18.25 g/L. The lowest yield of 6.10 g/L was observed at 45°C, at which temperature the γ -PGA producer exhibited the highest turbidimetric reading. In a related study, the optimal growth temperature for *Bacillus licheniformis* NRC20 was reported to be 30°C, while the highest γ -PGA yield was obtained at 35°C.^{16,21}

From Fig. 4, while the lowest γ -PGA production was recorded at an acidic pH (4.5), the highest was at pH 5.5 (26 g/L). At neutral pH and above, the γ -PGA yield was reduced to about 64% of the highest yield though the bacterial growth was highest. The highest fermentative production of γ -PGA was reported at a pH of 6.5.²² The level of pH significantly affects bacterial nutrient solubility and uptake, enzyme activity, and cell membrane morphology, thus impacting the formation of by-products (γ -PGA release).¹⁶ The fact that the highest γ -PGA yield was recorded at pH 5.5 may indicate that this pH influenced microbial metabolism to favor a higher γ -PGA release.

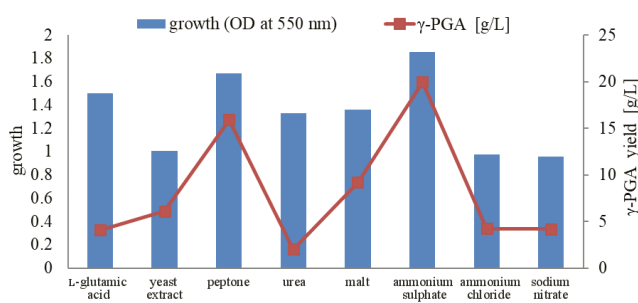


Fig. 2. Effect of different nitrogen sources on the growth and poly- γ -glutamic-acid (γ -PGA) yield of *Bacillus toyonensis* As8

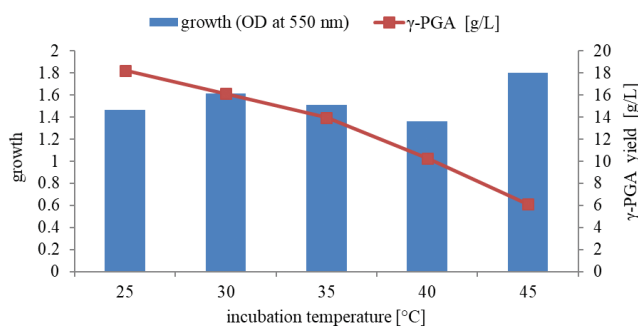


Fig. 3. Effect of incubation temperature on the growth and poly- γ -glutamic-acid (γ -PGA) yield of *Bacillus toyonensis* As8

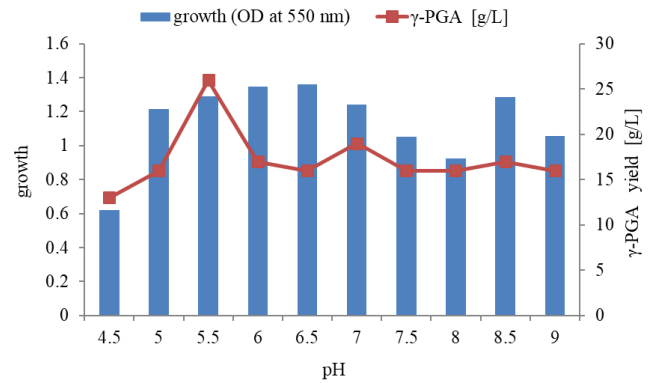


Fig. 4. Effect of pH on the growth and poly- γ -glutamic-acid (γ -PGA) production of *Bacillus toyonensis* As8

Effects of inoculant concentration and incubation period on γ -PGA production

Over the 96 h, bacterial growth increased in the 2 flask experiments. However, the highest γ -PGA yield (23.65 g/L) was observed after 48 h of incubation in the production medium inoculated with 10% of *B. toyonensis* As8. After this, there was a progressive reduction in yield from both media (Fig. 5A,B). Ju et al.¹⁹ reported the highest γ -PGA yield by a *B. subtilis* strain at the end of a 5-day incubation before a fall in yield and concluded that – for that strain – the longer the incubation time, the higher the production of γ -PGA. There was a progressive increase in optical density proportional to increasing incubation time. It was reported that the γ -PGA product could serve as a source of glutamate for the producing

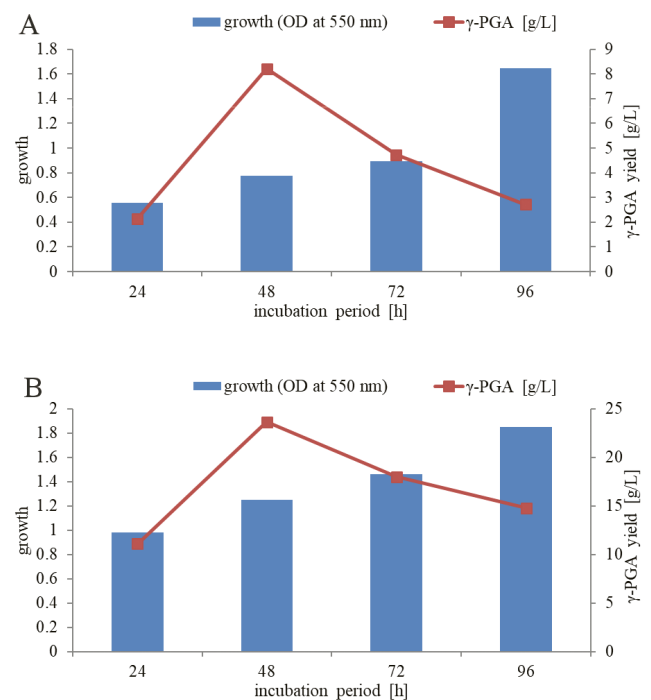


Fig. 5. Effect of (A) 1% and (B) 10% inoculation with different incubation periods on the growth and poly- γ -glutamic-acid (γ -PGA) production of *Bacillus toyonensis* As8

strain during its late stationary phase of life to sustain cell metabolism while nutrients and energy become limited,²³ which might be the reason for the reduction in the γ -PGA recovered. This also agrees with another report that the glutamic acid product of γ -PGA degradation catalyzed by γ -glutamyl hydrolase was utilized by the bacteria as a source of carbon and nitrogen.²⁴

γ -PGA production using agricultural residues

Many carbon- and nitrogen-based agro-industrial wastes (such as rice straw, wheat bran, corn bran, corn cob, sugarcane bagasse, cotton stalk, sorghum stover, and soybean cake) have been used as substrates in microbial fermentation because they can be biologically converted to 6-carbon and 5-carbon compounds which are funneled into the main carbon metabolism via glycolysis and the pentose phosphate pathway.^{20,25} Although all of the agro-substrates supported γ -PGA production, the highest yield was obtained with cassava peel (22.26 g/L) as the sole source of carbon (Table 2), an indication that the carbohydrate it contained could easily be metabolized by *B. toyonensis* As8 into simpler forms for subsequent conversion into α -ketoglutaric acid (a precursor metabolite of L-glutamine) in the citric acid cycle (TCA). There was an increase in γ -PGA production when 10% of the γ -PGA producer was cultivated under optimal culture conditions in a medium that now contained either cassava peel, fructose or Coix leaves with ammonium sulfate, at 25°C and a pH of 5.5, over 48 h to yield 26.45 g/L, 23.23 g/L and 16.87 g/L of γ -PGA, respectively.

Table 2. Effects of various agricultural wastes as carbon sources on poly- γ -glutamic-acid (γ -PGA) production by *Bacillus toyonensis* As8

Agro-waste – carbon source	γ -PGA [g/L]
Corn cob	6.03
Sorghum leaves	10.03
Coix noir leaves	8.37
Cassava peels	22.26
Rice bran	8.35

Characterization of the γ -PGA produced

Fourier transform infrared spectroscopy of the γ -PGA produced by *B. toyonensis* As8 revealed the key characteristic functional groups of γ -PGA (Fig. 6). The absorbance spectrum had peaks ranging from 441.26 cm^{-1} to 3771.78 cm^{-1} , where functional groups including hydroxyl, amide, carbonyl, and amine groups – common features of γ -PGA – were represented. This is similar to the results obtained by Kedia et al.,¹⁸ who measured over 100 scans and wavelength ranges of 400–4000 cm^{-1} using the same technique. The results of the present study for the γ -PGA produced by *B. toyonensis* As8 – amide absorption

at 1639.38 cm^{-1} , carbonyl absorption at 1439.00 cm^{-1} and hydroxyl absorption at 3417.00 cm^{-1} – are in agreement with those of other authors^{17,19,26} who independently reported a strong amide (N–H) absorption at ~1620–1655 cm^{-1} , a weaker carbonyl (C=O) absorption at ~1394–1454 cm^{-1} , a strong hydroxyl (OH) absorption at ~3400–3450 cm^{-1} , and a characteristically strong amine (C–N) absorption in the range of 1085–1165 cm^{-1} .

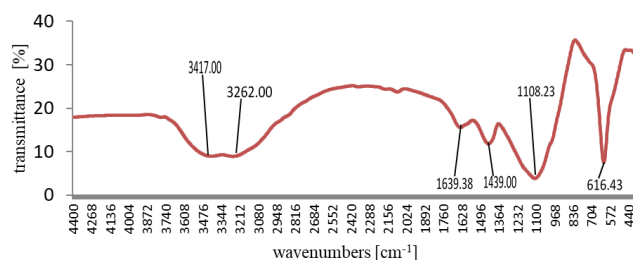


Fig. 6. FTIR Spectra of the poly- γ -glutamic-acid (γ -PGA) produced by *Bacillus toyonensis* As8

Figure 7 shows the scanning electron micrograph of the γ -PGA produced by *B. toyonensis* As8. The polymer particles were clumped together as agglomerates and the surfaces of the agglomerates were rough, wrinkled and non-uniform, which indicates the polymeric material might be non-free-flowing, loosely packed and porous.

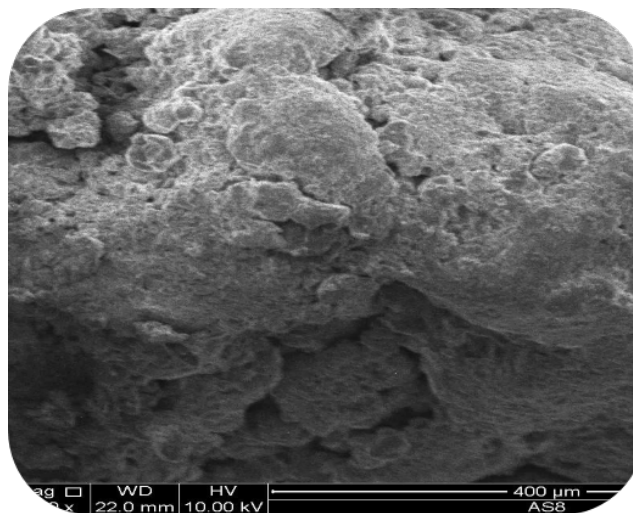



Fig. 7. Scanning electron micrograph of the poly- γ -glutamic-acid (γ -PGA) produced by *Bacillus toyonensis* As8


Conclusions

In this study, the effects of media components and various agricultural wastes as substrates for the microbial production of γ -PGA were investigated. Cassava peels as the sole source of carbon supported the highest γ -PGA yield for the non-glutamic-acid-dependent *Bacillus toyonensis* As8 (26.45 g/L) at a pH of 5.5 and at 25°C.

Also, the key groups/peaks present in the product were characteristic of the γ -PGA. Although they have been used in the past as substrates due to their abundance in our environment, cassava peels and many other agricultural by-products could be harnessed as substrates for large-scale γ -PGA production in a bid to reduce the high costs associated with commercial γ -PGA production.

ORCID iDs

Olubusola A. Odeniyi  <https://orcid.org/0000-0002-0826-791X>

David S. Avoseh  <https://orcid.org/0000-0002-0647-1546>

References

- Shih IL, Van YT. The production of poly (gamma-glutamic acid) from microorganisms and its various applications. *Bioresour Technol.* 2001;79(3):207–225.
- Sung MH, Park C, Kim CJ, Poo H, Soda K, Ashiuchi M. Natural and edible biopolymer poly- γ -glutamic acid: Synthesis, production, and applications. *Chem Rec.* 2005;5(6):352–366.
- Bajaj IB, Singhal RS. Poly (glutamic acid): An emerging biopolymer of commercial interest. *Bioresour Technol.* 2011;102(10):5551–5561.
- Sanda F, Fujiyama T, Endo T. Chemical synthesis of poly-gamma-glutamic acid by polycondensation of gamma-glutamic acid dimer: Synthesis and reaction of poly-gamma-glutamic acid methyl ester. *Polym Sci Chem.* 2001;39(5):732–741.
- Ogunleye A, Bhat A, Irorere VU, Hill D, Williams C, Radecka I. Poly- γ -glutamic acid: Production, properties and applications. *Microbiology.* 2015;161(Pt 1):1–17.
- Goto A, Kunioka M. Biosynthesis and hydrolysis of poly (γ -glutamic acid) from *Bacillus subtilis* IFO3335. *Biosci Biotechnol Biochem.* 1992;56(7):1031–1035.
- Candela T, Moya M, Haustant M, Fouet A. *Fusobacterium nucleatum*, the first Gram-negative bacterium demonstrated to produce polyglutamate. *Can J Microbiol.* 2009;55(5):627–632.
- Sakai K, Sonoda C, Murase K, inventors; Bitterness relieving agent. 2000. JP Patent WO0021390.
- Bhat AR, Irorere VU, Bartlett T, et al. Improving survival of probiotic bacteria using bacterial poly- γ -glutamic acid. *Int J Food Microbiol.* 2015;196:24–31.
- Luo Z, Guo Y, Liu J, et al. Microbial synthesis of poly- γ -glutamic acid: Current progress, challenges, and future perspectives. *Biotechnol Biofuels.* 2016;9(134):1–12.
- Olutiola PO, Famurewa O, Sonntag HG. *Introduction to General Microbiology: A Practical Approach.* 2nd ed. Ikeja, Nigeria: Bolabay Publications; 2000.
- Nagai T, Koguchi K, Itoh Y. Chemical analysis of poly- γ -glutamic acid produced by plasmid-free *Bacillus subtilis* (natto): Evidence that plasmids are not involved in poly- γ -glutamic acid production. *J Gen Appl Microbiol.* 1997;43(3):139–143.
- Kunioka M, Goto A. Biosynthesis of poly (γ -glutamic acid) from L-glutamic acid, citric acid, and ammonium sulfate in *Bacillus subtilis* IFO3335. *Appl Microbiol Biotechnol.* 1994;40(6):867–872.
- Fawole MO, Oso BA. *Characterization of Bacteria: Laboratory Manual of Microbiology.* 4th ed. Ibadan, Nigeria: Spectrum Book Ltd; 2004.
- Seo JH, Kim CS, Lee SP. Physicochemical properties of poly- γ -glutamic acid production by a novel *Bacillus subtilis* HA isolated from Cheonggukjang. *J Food Sci Nutr.* 2008;13(4):354–361.
- Tork SE, Aly MM, Alakilli SY, Al-Seeni MN. Purification and characterization of gamma poly glutamic acid from newly *Bacillus licheniformis* NRC20. *Int J Biol Macromol.* 2015;74:382–391.
- Ho GH, Ho TI, Hsieh KH, et al. γ -Polyglutamic acid produced by *Bacillus subtilis* (natto): Structural characteristics, chemical properties and biological functionalities. *J Chinese Chem Soc Taipei.* 2006;53(6):1363–1384.
- Kedia G, Hill D, Hill R, Radecka I. Production of poly-glutamic acid by *Bacillus subtilis* and *Bacillus licheniformis* with different growth media. *J Nanosci Nanotechnol.* 2010;10(9):5926–5934.
- Ju WT, Song YS, Jung WJ, Park RD. Enhanced production of poly- γ -glutamic acid by a newly-isolated *Bacillus subtilis*. *Biotechnol Lett.* 2014;36(11):2319–2324.
- Peng Y, Zhang T, Mu W, Miao M, Jiang B. Intracellular synthesis of glutamic acid in *Bacillus methylotrophicus* SK19.001, a glutamate independent poly (γ -glutamic acid)-producing strain. *J Sci Food Agric.* 2016;96(1):66–72.
- Du G, Yang G, Qu Y, Chen J, Lun S. Effects of glycerol on the production of poly (γ -glutamic acid) by *Bacillus licheniformis*. *Process Biochemistry.* 2005;40(6):2143–2147.
- Shih IL, Van YT, Chang YN. Application of statistical experimental methods to optimize production of poly(γ -glutamic acid) by *Bacillus licheniformis* CCRC 12826. *Enzyme and Microbial Technology.* 2002;31(3):213–220.
- Hezayen FF, Rehm BHA, Eberhardt R, Steinbuechel A. Polymer production by two newly isolated extremely halophilic *Archaea*: Application of a novel corrosion-resistant bioreactor. *Appl Microbiol Biotechnol.* 2000;54(3):319–325.
- Kimura K, Tran LSP, Uchida I, Itoh Y. Characterization of *Bacillus subtilis* γ -glutamyltransferase and its involvement in the degradation of capsule poly- γ -glutamate. *Microbiology.* 2004;150(Pt 12):4115–4123.
- Odeniyi OA, Adeola OJ. Production and characterization of polyhydroxyalkanoic acid from *Bacillus thuringiensis* using different carbon substrates. *Int J Biol Macromol.* 2017;104(Pt A):407–413.
- Bhat AR, Irorere VU, Bartlett T, et al. *Bacillus subtilis* natto: A non-toxic source of poly- γ -glutamic acid that could be used as a cryoprotectant for probiotic bacteria. *AMB Express.* 2013;3(36):1–9.

Formulation and solid state characterization of carboxylic acid-based co-crystals of tinidazole: An approach to enhance solubility

Jyotsana R. Madan^{1,A–F}, Rishikesh H. Dagade^{1,B–D,F}, Rajendra Awasthi^{2,A,C–F}, Kamal Dua^{3,A,C–F}

¹ Department of Pharmaceutics, Smt. Kashibai Navale College of Pharmacy, Savitribai Phule Pune University, India

² Amity Institute of Pharmacy, Amity University, Noida, India

³ Discipline of Pharmacy, Graduate School of Health, University of Technology, Sydney, Australia

A – research concept and design; B – collection and/or assembly of data; C – data analysis and interpretation; D – writing the article; E – critical revision of the article; F – final approval of the article

Polymers in Medicine, ISSN 0370-0747 (print), ISSN 2451-2699 (online)

Polim Med. 2018;48(2):99–104

Address for correspondence

Jyotsana R. Madan
E-mail: jyotsna.madan@sinhgad.edu

Funding sources

None declared

Conflict of interest

None declared

Received on July 22, 2018

Reviewed on January 23, 2019

Accepted on March 13, 2019

Cite as

Madan JR, Dagade RH, Awasthi R, Dua K. Formulation and solid state characterization of carboxylic acid-based co-crystals of tinidazole: An approach to enhance solubility. *Polim Med.* 2018;48(2):99–104. doi:10.17219/pim/105609

DOI

10.17219/pim/105609

Copyright

© 2019 by Wrocław Medical University

This is an article distributed under the terms of the

Creative Commons Attribution 3.0 Unported (CC BY 3.0)

(<https://creativecommons.org/licenses/by/3.0/>)

Abstract

Background. Tinidazole (TNZ) is an anti-parasite drug used in the treatment of a variety of amebic and parasitic infections. It has low solubility in aqueous media and is categorized under Class II of the Biopharmaceutical Classification System.

Objectives. The aim of this research was to study the potential for enhancing the solubility of TNZ using carboxylic acid co-crystals.

Material and methods. The solubility of TNZ was determined individually using 6 carboxylic acids for forming co-crystals at a 1:1 stoichiometric ratio. Three carboxylic acids – namely tartaric acid (TA), oxalic acid (OA) and glutaric acid (GA) – resulted in the formation of co-crystals with enhanced solubility. An equilibrium solubility study of TNZ co-crystals at 1:1.5 and 1:2 stoichiometric ratios was also carried out. The co-crystals which developed were evaluated using X-ray powder diffraction (XRD) and differential scanning calorimetry (DSC) to study the drug–co-crystal former interactions.

Results. The solubility of TNZ in distilled water was found to be 0.014 mg/mL. The highest enhancement ratio was obtained with TNZ and TA at a ratio of 1:1. Differential scanning calorimetry thermograms suggested that the drug and carboxylic acids had undergone interactions such as hydrogen bonding. The XRD and DSC results confirmed the formation of co-crystals.

Conclusions. It was concluded that the results of enhanced solubility of TNZ using co-crystals is a clear indication of the potential for co-crystals to be used in the future for other poorly water-soluble drugs, considering that co-crystals are a safe and cost-effective approach.

Key words: solubility, co-crystals, solvent evaporation

Introduction

Pharmaceutical co-crystals are multi-component crystals based on hydrogen bonds without the transfer of hydrogen ions to form salts.¹ Co-crystal formation has recently gained attention in pharmaceutical applications. The ability to tailor the physicochemical properties of a substance via complexation is highly desirable in terms of dissolution rate, bioavailability, stability, and processing.^{2–5} Co-crystals can also enhance the flowability, compressibility and hygroscopicity of drugs.⁶ A co-crystal may be defined as a material which contains 2 or more discrete molecular entities in its crystal lattice.⁷ In pharmaceutical terms, a co-crystal is a molecular complex of an active pharmaceutical ingredient and a second molecule, known as a co-crystal former, which typically requires complementary hydrogen bonding between the 2 components.⁸ Co-crystallization may influence the pharmacokinetics of therapeutically active compounds, which may in turn influence their biopharmaceutical and bioavailability properties, including absorption.^{9–11} The components in a co-crystal exist in a definite stoichiometric ratio, and are assembled via non-covalent interactions such as hydrogen bonds, ionic bonds, π - π , or van der Waals interactions rather than by ion pairing.¹²

Tinidazole [1-(2-ethylsulfonyl)ethyl]-2-methyl-5-nitroimidazole (TNZ) (Fig. 1) is an anti-parasite drug used against protozoan infections. It may also be used as part of a combination therapy for *Helicobacter pylori* eradication. It has low solubility in aqueous media and is categorized as Class II in the Biopharmaceutical Classification System.¹³ This property makes the drug a suitable candidate for research investigating new salts with improved solubility.

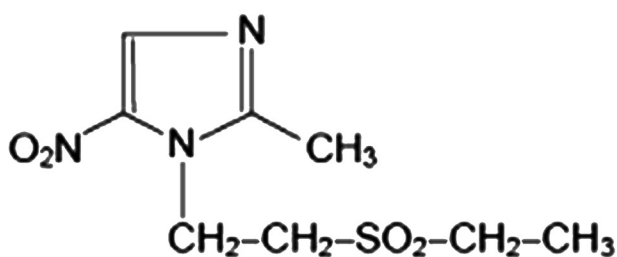


Fig. 1. Chemical structure of TNZ

The aim of this work was to explore the possibility of TNZ co-crystal formation with various carboxylic acids, with an emphasis on determining whether it can form co-crystals with multiple stoichiometries. A method based on solvent evaporation was used to determine the possibility of forming co-crystals from the 2 components.

The spherical crystallization technique is a novel agglomeration method for liquid systems which was developed by Kawashima in the 1980s.¹ In this system,

agglomeration and spheroidization can be carried out simultaneously during the crystallization process of a substance with a bridging liquid by means of stirring. In the beginning, the spherical crystallization technique was mainly used in direct tableting technology because crystallization and agglomeration could be carried out simultaneously in a single step. The resultant agglomerates exhibited dramatically improved flowability, packability and compressibility.^{2,3} Later on, functional drug devices such as microspheres,⁴ microcapsules,⁵ microballoons,⁶ and biodegradable nanospheres⁷ were developed using the emulsion-solvent-diffusion method, one of the spherical crystallization techniques involving the introduction of a functional polymer into the system.

Material and methods

Material

The TNZ was received as a gift sample by Aarti Drugs Ltd., Mumbai, India. Tartaric acid (TA), oxalic acid (OA), glutaric acid (GA), citric acid, salicylic acid, malonic acid, magnesium stearate, talc, and lactose monohydrate were purchased from Research-Lab Fine Chem Industries, Mumbai, India. Sodium starch glycolate and microcrystalline cellulose were purchased from BASF India Ltd., Mumbai, India. Methanol was purchased from Thomas Baker Chemicals, Mumbai, India. All other reagents were of analytical grade.

Methods

Determination of solubility

The saturation solubility of TNZ was determined in distilled water. In brief, 100 mg of TNZ was added to the distilled water and kept in an incubator shaker (100 rpm) for 24 h at 37°C. After 24 h, the solution was centrifuged at 2000 rpm for 15 min and filtered through Whatman grade 41 filter paper. The supernatant was diluted with distilled water and its absorbance was measured at 318 nm using a UV spectrophotometer (model V-630; Shimadzu Corporation, Kyoto, Japan). The saturation solubility was then calculated.

Preliminary trials for the preparation of TNZ co-crystals

Based on the literature,^{14–18} 6 carboxylic acids were initially selected for producing co-crystals of TNZ at a 1:1 stoichiometric ratio. In brief, a precisely weighed amount of TNZ and individual carboxylic acids (TA, OA, GA, malonic acid, salicylic acid, and citric acid) at a 1:1 stoichiometric ratio were dissolved in methanol and sonicated for 10 min in order to completely mix the ingredients. The resulting solution was poured onto a Petri plate and stored

to allow the solvent to completely evaporate at room temperature (25°C). Co-crystals of TNZ formed with 3 of the carboxylic acids (TA, OA and GA). No co-crystals were obtained from malonic acid, salicylic acid or citric acid. Based on these results, TA, OA and GA were selected for further study and were used to produce TNZ co-crystals at 1:1.5 and 1:2 stoichiometric ratios (Table 1).

Equilibrium solubility study of TNZ co-crystals (1:1, 1:1.5, and 1:2 stoichiometric ratios)

The solubility of TNZ in water from co-crystals formed with the 3 carboxylic acids remaining after screening (TA, OA and GA) was determined at room temperature using an incubator shaker (OS-02; Chromus Biotech, Bengaluru, India). Excess amounts of the TNZ co-crystals with the individual carboxylic acids at different ratios (Table 2) were added to 5 mL of distilled water and were shaken until a saturated solution was formed. The vials were shaken on a mechanical shaker for 24 h. The solution was then centrifuged at 2000 rpm for 10 min in an ultra-centrifuge and were filtered through Whatman grade 41 filter paper. Aliquots were suitably diluted with distilled water and methanol (1:1) and analyzed using a UV spectrophotometer (model V-630; Shimadzu Corporation) at 318 nm.

Characterization of TNZ co-crystals

Differential scanning calorimetry (DSC)

To investigate the effect of temperature, thermograms of TNZ, TA, OA and GA, as well as of co-crystals of TNZ and the 3 carboxylic acids were recorded using a differential scanning calorimeter (DSC 4000 System; Perkin Elmer, Waltham, USA). An empty aluminum pan was used as a reference. The DSC measurements were taken at a heating rate of 10°C/min from 30°C to 300°C.^{19,20}

Table 1. Results of solubility studies for TNZ–carboxylic acid co-crystals

Drug	Carboxylic acid	Quantity of drug [mg]	Quantity of carboxylic acid [mg]	Solubility [mg/mL]*	Solubility enhancement ratio
1:1 stoichiometric ratio					
TNZ	tartaric acid	200	121.39	0.1540 ±0.002	11.00
TNZ	oxalic acid	200	72.81	0.0700 ±0.001	5.00
TNZ	glutaric acid	200	106.85	0.0784 ±0.001	5.60
1:1.5 stoichiometric ratio					
TNZ	tartaric acid	200	182.08	0.0995 ±0.002	7.10
TNZ	oxalic acid	200	109.22	0.1445 ±0.003	10.32
TNZ	glutaric acid	200	160.28	0.1183 ±0.002	8.45
1:2 stoichiometric ratio					
TNZ	tartaric acid	200	242.78	0.0995 ±0.001	1.12
TNZ	oxalic acid	200	145.62	0.1445 ±0.002	3.41
TNZ	glutaric acid	200	213.70	0.0160 ±0.001	1.18

* Data is presented as mean ± standard deviation (SD) (n = 3).

Table 2. Formulation of TNZ tablets prepared by the direct-compression method (formulation T1)

Ingredients	Quantity [mg]
Co-crystal equivalent of 300 mg of tinidazole with tartaric acid (1:1)	482
Microcrystalline cellulose	60
Sodium starch glycolate	12
Magnesium stearate	8
Talc	8
Lactose	150

X-ray powder diffraction analysis

The physical state of pure TNZ and TNZ in co-crystals was examined using an X-ray diffraction analyzer (Philips 1710 powder X-ray diffractometer; Koninklijke Philips N.V., Amsterdam, the Netherlands). The X-ray diffraction patterns were recorded using CuK α radiations ($\theta = 1.54059 \text{ \AA}$), a current of 30 mA, and a voltage of 40 kV. The samples were analyzed over a 2θ range of 10–80.^{21–23}

In vitro dissolution study

The drug dissolution rates from different co-crystals were determined and compared to that of pure TNZ. The dissolution study was performed using a United States Pharmacopeia (USP) type-II apparatus (model TDT-08L; Electrolab India, Mumbai, India). The dissolution medium (900 mL of distilled water) was maintained at a temperature of $37 \pm 0.5^\circ\text{C}$ in the dissolution vessel. The co-crystal equivalent of 300 mg of TNZ was placed into the dissolution vessel and the paddle was rotated at 50 rpm. Aliquots were withdrawn at 15 min intervals for 90 min. Those samples were filtered and analyzed using a UV spectrophotometer (model V-630; Shimadzu Corporation) at 318 nm. The dissolution study was conducted in triplicate.^{19,20}

Production of TNZ tablets by the direct-compression method

Tablets of co-crystal equivalents of 300 mg of TNZ and TA (1:1) were prepared using the direct-compression method according to the formula given in Table 2. All of the ingredients were passed separately through a 60-mesh sieve. Co-crystals and microcrystalline cellulose were mixed by adding small amounts of each several times and blending them to obtain a uniform mixture and kept aside. The ingredients were then weighed and mixed in geometrical order and the tablets were compressed with a Rimek Compression Machine using the 8-millimeter flat round punch. The resulting tablets were evaluated and the pre-compression and post-compression parameters were compared.

In vitro drug release study

The in vitro drug release from the resulting tablets was studied using a USP type-II apparatus (USP XXIII Dissolution Test Apparatus; Electrolab India, Mumbai, India) at 100 rpm using 900 mL of distilled water as a release medium. The temperature of the medium was maintained at $37 \pm 0.5^\circ\text{C}$. Aliquots were withdrawn at 30-minute intervals for 180 min, then filtered and analyzed at 318 nm using a UV spectrophotometer (model V-630; Shimadzu Corporation). The drug concentration was determined from the standard calibration curve. The release profile of a commercially available TNZ tablet (300 mg of TNZ – Tiniba 300 tablet; Zydus Cadila, Ahmadabad, India) was compared with that of the tablets produced.

Results and discussion

Some of the acids (TA, OA and GA) provided satisfactory results in terms of safety for acceptance in therapy (Fig. 2). Hydrogen bonds occur between the nitrogen and sulfonyl oxygen of TNZ and the hydrogen of the hydroxyl group of TA. When it comes to OA and GA, the formation of hydrogen bonds between these atoms may not be favorable. The 2 carbon atoms separating the carboxyl groups (-COOH) from the hydrogen-bond donor hydroxyl groups in TA may be optimally suited to form such hydrogen bonds, whereas the 3 carbon atoms separating the carboxyl groups (-COOH) in GA – or 0 carbon atoms in the case of

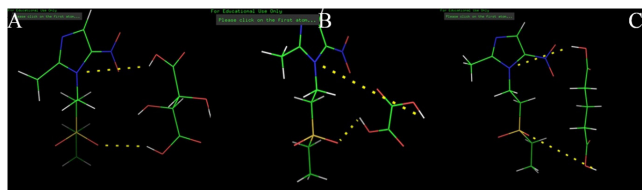


Fig. 2. The probable hydrogen bond formation between TNZ and tartaric acid (A), TNZ and oxalic acid (B), and TNZ and glutaric acid (C)

OA – may be less favorable than TA. The stronger ability of TA to form hydrogen bonds with TNZ may be responsible for the enhanced solubility of these co-crystals.

Equilibrium solubility studies of the co-crystals

The solubility of TNZ in distilled water was found to be 0.014 mg/mL. Co-crystals of TNZ and tartaric acid demonstrated maximum solubility at a stoichiometric ratio of 1:1, while OA and GA co-crystals performed best at a ratio of 1:1.5. The solubility enhancement ratios of the above combinations were 11.00 (TNZ:TA, 1:1), 10.32 (TNZ:OA, 1:1.5), and 8.45 (TNZ:GA, 1:1.5), respectively (Table 1).

Differential scanning calorimetry analysis

As the physical state of a drug influences its release kinetics, differential scanning calorimetry (DSC) was conducted for the pure drug, for carboxylic acids and for the co-crystals in order to determine the physical state of drug – i.e., amorphous or crystalline – before and after the production of co-crystals. The results of the DSC study are presented in Fig. 3. The DSC spectrum of TNZ showed a sharp endothermic peak at 128°C , indicating its melting point ($126\text{--}129^\circ\text{C}$). In the DSC thermogram of the co-crystals with enhanced solubility (TNZ:TA, 1:1, TNZ:OA, 1:1.5 and TNZ:GA, 1:1.5), the endothermic peaks of both the drug and the carboxylic acids (TA, OA and GA) were visible, but not very intense and slightly shifted from their original positions, indicating that the TNZ and the carboxylic acids had undergone interactions such as hydrogen bonding.

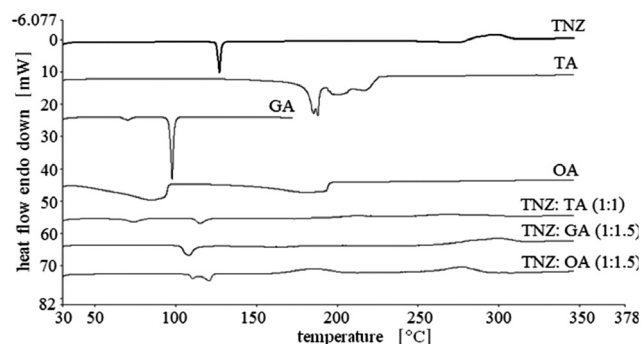


Fig. 3. Differential scanning calorimetry analysis (DSC) of TNZ and co-crystals

X-ray powder diffraction analysis

X-ray diffraction was used to evaluate the physical state of TNZ and the drug within the co-crystals produced. The X-ray diffractograms of TNZ, the carboxylic acids and the co-crystals are presented in Fig. 4. Tinidazole displayed characteristic, intense peaks at 2θ of 10.62, 15.24, 17.84, 18.18, 18.84, 21.23, 22.42, 23.87, 27.20, 27.63, 28.28, 29.57, 31.28, 33.15, 35.26, 36.26, 37.26, 38.26, 31.21, 34.24, and 39.46° , indicating its crystalline nature.

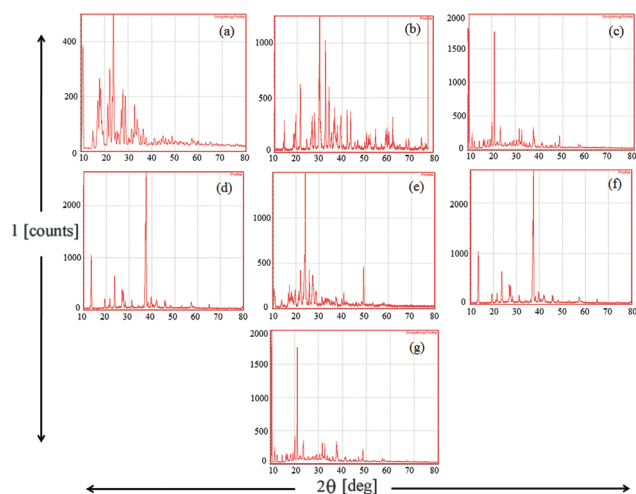


Fig. 4. X-ray powder diffraction (XRPD) spectra of (a) TNZ, (b) tartaric acid, (c) TNZ + tartaric acid (1:1), (d) glutaric acid, (e) TNZ + glutaric acid (1:1.5), (f) oxalic acid, and (g) TNZ + oxalic acid (1:1.5)

In the co-crystals prepared with TA, peaks of a reduced intensity were visible at 2θ of 11.39, 13.92, 15.84, 17.93, 18.17, 19.42, 20.34, 21.14, 23.42, 32.34, 33.17, and 37.52, indicating that the drug is partly dissolved within the formed matrix and partly in an amorphous form distributed throughout the system.

The co-crystals with GA showed peaks at 2θ of 10.62, 13.94, 17.24, 18.44, 19.14, 22.22, 24.24, 26.42, 25.13, 29.31, 37.41, 41.16, and 49.46, while the co-crystals with OA demonstrated peaks at 2θ of 10.12, 11.95, 12.87, 14.24, 16.14, 17.24, 18.24, 19.57, 20.11, 21.22, 23.24, 29.42, 30.23, 31.37, 32.21, 37.86, and 49.34. Overall, the decrease in the number and intensity of peaks indicates that the drug is partly dissolved within the formed matrix and partly in a crystalline form distributed throughout the system; this confirms the formation and existence of co-crystals.

Dissolution profile of TNZ and TNZ co-crystals at different stoichiometric ratios

The dissolution profiles of TNZ and co-crystals of TNZ with different carboxylic acids and at different stoichiometric ratios are presented in Fig. 5–7. From the equilibrium

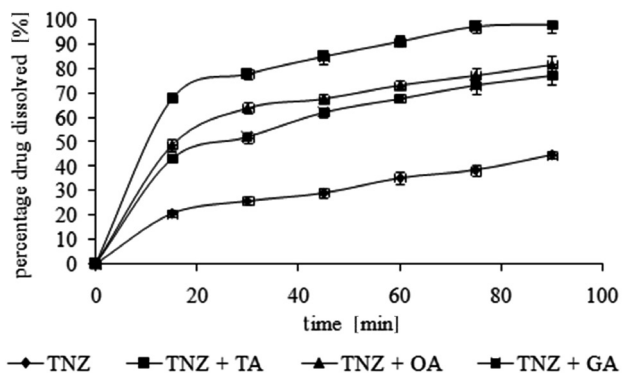


Fig. 5. Dissolution profile of TNZ and TNZ co-crystals (1:1 ratio) in distilled water at $37^{\circ}\text{C} \pm 0.5^{\circ}\text{C}$ (data presented as mean \pm SD, $n = 3$)

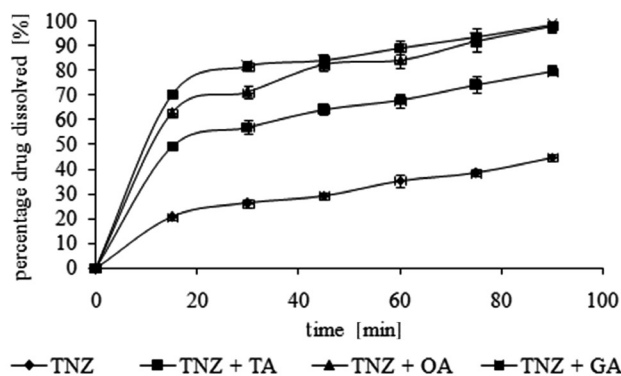


Fig. 6. Dissolution profile of TNZ and TNZ co-crystals (1:1.5 ratio) in distilled water at $37^{\circ}\text{C} \pm 0.5^{\circ}\text{C}$ (data presented as mean \pm SD, $n = 3$)

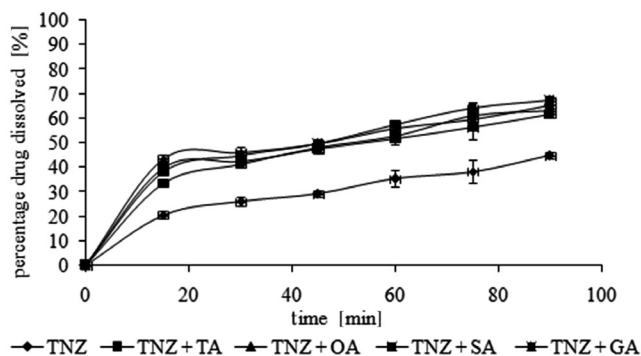


Fig. 7. Dissolution profile of TNZ and co-crystals of TNZ (1:2 ratio) in distilled water at $37^{\circ}\text{C} \pm 0.5^{\circ}\text{C}$ (data presented as mean \pm SD, $n = 3$)

solubility studies and dissolution studies, it was determined that a 1:1 stoichiometric ratio is best for TNZ + TA co-crystals. A 1:1.5 stoichiometric ratio was found to be best for TNZ + OA and TNZ + GA co-crystals. The analysis indicates that TNZ + TA (1:1 stoichiometric ratio) performed the best of all the ratios, and was therefore selected for the production of tablets.

Evaluation of tablets

Pre-compression parameters

The small differences in the values of bulk density and tapped density illustrate the free-flowing nature of powder blend. Hausner’s ratio was found to be 1.132, which indicates that the powder blend is free-flowing (Table 3). The value of compressibility index (15–16) and the angle of repose ($30\text{--}31^{\circ}$) indicate good flowability, so the powder blend can be used to directly manufacture directly compressed tablets.

Table 3. Results of pre-compression powder blend (formulation T1); the data is presented as mean \pm standard deviation (SD) ($n = 3$)

Bulk density [gm/cm ³]	Tapped density [gm/cm ³]	Hausner ratio	Compressibility index [%]	Angle of repose [°]
0.845 \pm 0.04	0.926 \pm 0.08	1.132 \pm 0.06	16.30 \pm 1.26	31.00 \pm 1.45

Post-compression parameters

The post-compression parameters of the tablets containing TNZ–carboxylic acid co-crystals (formulation T1) are as follows: the hardness of the tablets was 2.00 ± 0.14 kg/cm², their friability was $0.61 \pm 0.01\%$, the drug content was $97 \pm 0.82\%$, and the disintegration time was 120 ± 5 s (Table 4). All of the post-compression parameters were within the acceptable ranges.

Table 4. Results of TNZ tablets (formulation T1); the data is presented as mean \pm standard deviation (SD) (n = 3)

Hardness [kg/cm ²]	Friability [%]	Drug content [%]	In vitro disintegration time [s]
2.00 \pm 0.14	0.61 \pm 0.01	97.00 \pm 0.82	120 \pm 5

In vitro release studies

Figure 8 presents a graph comparing the percentage of cumulative TNZ release over time for the tablets produced in this study vs a commercially available formulation. The results indicate that after 2 h, the cumulative percentage release of formulation T1 was greater (74.23%) than that of the tablets available on the market (48.42%).

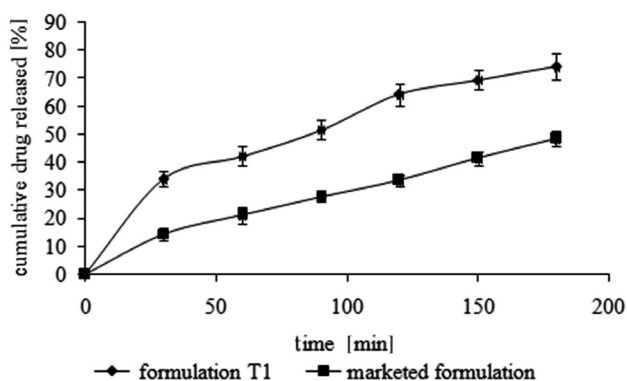


Fig. 8. Comparison of release profile of prepared tablet with marketed tablet in distilled water at $37^\circ\text{C} \pm 0.5^\circ\text{C}$ (data presented as mean \pm SD, n = 3)

Conclusions

Our study has clearly revealed that the application of carboxylic acid co-crystals is an effective and safe approach to increasing the dissolution rate of poorly water-soluble drugs. We have demonstrated the utility of carboxylic acid co-crystals using a practically insoluble drug, TNZ, which is a clear indication of their potential application in various other poorly water-soluble drugs.

ORCID iDs

Jyotsana R. Madan <https://orcid.org/0000-0001-6663-1890>
 Rishikesh H. Dagade <https://orcid.org/0000-0001-6071-373X>
 Rajendra Awasthi <https://orcid.org/0000-0002-1286-1874>
 Kamal Dua <https://orcid.org/0000-0002-7507-1159>

References

1. Yadav AV, Shete AS, Dabke AP, Kulkarni PV, Sakhare SS. Co-crystals: A novel approach to modify physicochemical properties of active pharmaceutical ingredients. *Indian J Pharm Sci.* 2009;71(4):359–370.
2. Basavoju S, Bostrom D, Velaga SP. Pharmaceutical cocrystal and salts of norfloxacin. *Crys Growth Des.* 2006;6(12):2699–2708.
3. Shiraki K, Takata N, Takano R, Hayashi Y, Terada K. Dissolution improvement and the mechanism of improvement from co-crystallization of poorly water-soluble compounds. *Pharm Res.* 2008;25(11):2581–2592.
4. Trask AV, Motherwell WDS, Jones W. Physical stability enhancement of theophylline via co-crystallization. *Int J Pharm.* 2006;320(1–2):114–123.
5. Sun CC, Hou H. Improving mechanical properties of caffeine and methyl gallate crystal by co-crystallization. *Crys Growth Des.* 2008;8(5):1575–1579.
6. Schultheiss N, Newman A. Pharmaceutical co-crystals and their physicochemical properties. *Cryst Growth Des.* 2009;9(6):2950–2967.
7. Trask AV, Jones W. Crystal engineering of organic co-crystals by the solid state grinding approach. *Top Curr Chem.* 2005;254:41–70.
8. McNamara DP, Childs SL, Giordano J, et al. Use of a glutaric acid cocrystal to improve oral bioavailability of a low solubility API. *Pharm Res.* 2006;23(4):1888–1897.
9. Aakeroy CB, Salmon DJ. Building co-crystals with molecular sense and supramolecular sensibility. *Cryst Eng Comm.* 2005;7(72):439–448.
10. Miroshnyk I, Mirza S, Sandler N. Pharmaceutical co-crystals: An opportunity for drug product enhancement. *Expert Opin Drug Deliv.* 2009;6(4):333–341.
11. McMahon JA. Crystal engineering of novel pharmaceutical forms. Master of Science Thesis, Department of Chemistry, University of South Florida, USA, 2006.
12. Zaworotko M. Crystal engineering of co-crystals and their relevance to pharmaceuticals and solid-state chemistry. *Acta Cryst.* 2008;64(a1):C11–C12.
13. Jagdale S, Kulkarni A, Chabukswar A, Kuchekar B. Design and evaluation of microwave induced solid dispersion of tinidazole and molecular modelling with β -cyclodextrin. *Lett Drug Des Discov.* 2016;13(8):781–792.
14. Rodríguez-Hornedo N, Nehm SJ, Jayasankar A. Cocrystals. Design, properties and formation mechanisms. In: *Encyclopedia of Pharmaceutical Technology*. 3rd ed. London, UK: Taylor & Francis; 2007:615–635.
15. Vishweshwar P, McMahon JA, Bis JA, Zaworotko MJ. Pharmaceutical co-crystals. *J Pharm Sci.* 2006;95(3):499–516.
16. Alatas F, Rathi H. Enhancement of solubility and dissolution rate enhancement of telmisartan by TMS-oxalic acid co-crystal formation. *Int J Pharm Pharm Sci.* 2015;7(3):423–426.
17. Shah K, Borhade S, Londhe V. Utilization of co-crystallization for solubility enhancement of poorly water soluble drug – Ritonavir. *Int J Pharm Pharm Sci.* 2014;6(2):556–558.
18. Masuda T, Yoshihashi Y, Yonemochi E, Fujii U, Uekusa H, Terada K. Co-crystallization and amorphization induced by drug-excipient interaction improves the physical properties of acyclovir. *Int J Pharm.* 2012;422(1–2):160–169.
19. Madan JR, Kamate VJ, Awasthi R, Dua K. Formulation, characterization and in-vitro evaluation of fast dissolving tablets containing gliclazide hydrotropic solid dispersions. *Recent Pat Drug Deliv Formul.* 2017;11(2):147–154.
20. Madan JR, Pawar KT, Dua K. Solubility enhancement studies on lurasidone hydrochloride using mixed hydrotropy. *Int J Pharm Invest.* 2015;5(2):114–120.
21. Malipeddi VR, Dua K, Awasthi R. Development and characterization of solid dispersion-microsphere controlled release system for poorly water-soluble drug. *Drug Deliv Transl Res.* 2016;6(5):540–550.
22. Gorajana A, Rajendran A, Yew LM, Dua K. Preparation and characterization of cefuroxime axetil solid dispersions using hydrophilic carriers. *Int J Pharm Invest.* 2015;5(3):171–178.
23. Gorajana A, Kit WW, Dua K. Characterization and solubility study of norfloxacin-polyethylene glycol, polyvinylpyrrolidone and carbopol 974P solid dispersions. *Recent Pat Drug Deliv Formul.* 2015;9(2):167–182.

Polimery w Medycynie
Polymers in Medicine

